

The role of lipid particle-laden interfaces in regulating the co-delivery of two hydrophobic actives from o/w emulsions

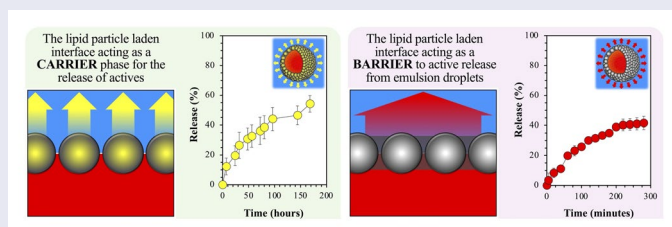
Georgia I. Sakellari^a, Hannah Batchelor^b and Fotis Spyropoulos^a

^aSchool of Chemical Engineering, University of Birmingham, Birmingham, UK; ^bStrathclyde Institute of Pharmacy and Biomedical Sciences, University of Strathclyde, Glasgow, UK

ABSTRACT

Co-delivery strategies have become an integral active delivery approach, although understanding of how the microstructural characteristics could be deployed to achieve independently regulated active co-delivery profiles, is still an area at its infancy. Herein, the capacity to provide such control was explored by utilizing Pickering emulsions stabilized by lipid particles, namely solid lipid nanoparticles (SLNs) and nanostructured lipid carriers (NLCs). These dual functional species, regarding their concurrent Pickering stabilization and active carrying/delivery capabilities, were formulated with different solid lipid and surfactant types, and the effect on the release and co-release modulation of two hydrophobic actives separately encapsulated within the lipid particles themselves and within the emulsion droplets was investigated. Disparities between the release profiles from the particles in aqueous dispersions or at an emulsion interface, were related to the specific lipid matrix composition. Particles composed of lipids with higher oil phase compatibility of the emulsion droplets were shown to exert less control over their release regulation ability, as were particles in the presence of surfactant micelles in the continuous phase. Irrespective of their formulation characteristics, all particles provided a level of active release control from within the emulsion droplets, which was dependant on the permeability of the formed interfacial layer. Specifically, use of a bulkier particle surfactant or particle sintering at the droplet interface resulted in more sustained droplet release rates. Compared to sole release, the co-release performance remained unaffected by the co-existence of the two hydrophobic actives with the co-release behavior persisting over a storage period of 1 month.

GRAPHICAL ABSTRACT



ARTICLE HISTORY

Received 22 June 2024
Revised 24 October 2024
Accepted 29 October 2024
2024

KEYWORDS

Solid lipid nanoparticles; nanostructured lipid carriers; Pickering emulsions; co-encapsulation; co-release; interfacial sintering

1. Introduction

Within the encapsulation and release research area, a range of different approaches have been explored to allow, facilitate and control the co-encapsulation and co-delivery of multiple actives. At the same time, the emergence of novel techniques to prepare such functional systems that can expedite controlled and targeted active delivery has been generating exciting possibilities for the optimization of such complex structures with diverse characteristics (Shrimal et al., 2020; Zhao et al., 2022a). Majority of the published work stems from and pertains to pharmaceuticals (Kolishetti et al., 2010; Meng et al., 2016; Kim et al., 2019; Motevalli et al., 2019), although co-delivery formulations have also found applications in

agrochemicals (Cui et al., 2020; Graily Moradi et al., 2019), cosmetics (Han et al., 2020) and food products (Wei et al., 2020; Chawda et al., 2017). Incorporating more than one active ingredient within the same formulation platform has been shown to enhance efficacy and bioactivity through synergistic or additive effects between the encased species (Tavano et al., 2014; Liu et al., 2019). To this end, solid-phase formulations have been primarily investigated (Lee et al., 2019; Wang et al., 2019; Awad et al., 2019), with less attention given to liquid-based systems, despite the associated advantages that the latter can provide; in the pharmaceuticals space, these would include dosage flexibility, rapid absorption and improved patient compliance (particularly for patients unable

CONTACT Georgia I. Sakellari  gis823@alumni.bham.ac.uk

© 2024 The Author(s). Published by Informa UK Limited, trading as Taylor & Francis Group. This is an Open Access article distributed under the terms of the Creative Commons Attribution License (<http://creativecommons.org/licenses/by/4.0/>), which permits unrestricted use, distribution, and reproduction in any medium, provided the original work is properly cited. The terms on which this article has been published allow the posting of the Accepted Manuscript in a repository by the author(s) or with their consent.

to swallow solids) (Helal et al., 2019; Čejková & Štěpánek, 2013; Li et al., 2016).

Among the approaches utilized for multi-delivery from liquid formulations, emulsions and specifically Pickering emulsions have emerged as attractive co-delivery vehicles, due to their capacity to bestow compartmentalized encapsulation and independently controlled delivery of the incorporated actives, as well as improved emulsion stabilization. Particulates of varying physicochemical characteristics have been explored, with most studies primarily focusing on confirming the concurrent stabilization and co-encapsulation aptitude of the systems. Sun *et al.* (Sun et al., 2022) studied the co-encapsulation of three active ingredients with different solubilities, namely vitamin B₂, vitamin E and β -carotene within liposome-stabilized emulsions, highlighting the impact of the microstructural components' composition on the obtained encapsulation efficiency. With regard to the effect of co-encapsulation on the system's properties, Chen et al. (2022) demonstrated that no obvious changes are inflicted to the size distribution of the blank emulsion, and overall improved stability following the co-incorporation of chlorogenic acid and β -carotene in shrimp ferritin nanocage-stabilized emulsions. In another work by Spyropoulos et al. (2018), the influence of the particles' characteristics on attaining independent and triggered co-delivery of a hydrophobic/hydrophilic active combination from emulsions stabilized by sodium caseinate/chitosan co-precipitated complexes was highlighted. It was shown that the hydrophilic model active encapsulated within the particles exhibited a (pH) triggered-release behavior, compared to the sustained discharge of the hydrophobic active encased within the emulsion droplets.

However, the crucial role of particle-laden interfaces on the co-release performance of such Pickering emulsion-based co-delivery systems is practically unexplored in current literature. Han et al. (2021) reported that the encapsulation of a secondary active (quercetin) within black bean protein-based nanocomplexes led to more sustained release rate of the (primary) active (perilla oil) contained within the Pickering emulsion droplets, due to the creation of thicker interfacial coating, compared to blank particles. In another study, the utilization of solid lipid nanoparticles (SLNs) fabricated with a bulkier protein as the surface active species resulted in minimal release from the particles, while creation of a less permeable interfacial layer due to sintering of the SLNs led to negligible discharge of a secondary active incorporated within the oil droplets (Sakellari et al., 2021b). In a slightly different iteration of the same principle, the potential to control the active release from w/o emulsions by manipulating the architecture of their lipid-decorated interfaces via sintering, was shown to lead to triggered release, through temperature control (Garrec et al., 2012; Frasc-Melnik et al., 2010). However, such an approach whereby the production of Pickering entities is fine-tuned prior to emulsion formation and their sintering is attuned *in-situ* at the droplet interface to achieve bespoke active release performances, is yet to be explored within a co-delivery setting.

The current work aimed to investigate the role of lipid particle-laden emulsion interfaces in terms of regulating the co-delivery performance of Pickering o/w emulsions (Sakellari

et al., 2022, 2023). The effect of formulation characteristics of the lipid particles, both SLNs and nanostructured lipid carriers (NLCs), on their simultaneous emulsion stabilization and active carrying/release regulation capabilities were studied. The release profiles of a model hydrophobic active (curcumin) encapsulated within SLNs and NLCs of varying formulations aspects, namely the types of solid lipid and surfactant used (during particle fabrication), were assessed in two settings; firstly, when the particles are simply dispersed in an aqueous medium (aqueous dispersions) and secondly, when the particles are (predominantly) positioned at an emulsion interface. Focus was also placed on examining the capacity and extent to which (blank) lipid particle interfaces could act as effective interfacial barriers and provide control over the encasing and release of a secondary model hydrophobic active (cinnamaldehyde) encapsulated within the (lipid particle-stabilized) o/w emulsion droplets; release behavior in this case was compared to that of simple (surfactant-stabilized) emulsions. Interfacial sintering was devised as a means to manipulate the interfacial barrier provided by the lipid particles and scrutinize how and to what degree this could provide further control over the release of the secondary active. Finally, the co-release of both model hydrophobic actives from SLN and NLC particle-stabilized emulsions was studied to confirm the co-encapsulation and co-delivery functionality of the developed formulation.

2. Materials and methods

2.1. Materials

Compritol[®] 888 ATO (C888, glyceryl behenate) and Precirol[®] ATO 5 (P5, glyceryl palmitostearate) were kindly provided from Gattefossé (Saint-Priest, France). Miglyol[®] 812 (medium chain triglycerides, MCTs) was a kind gift from IOI Oleo (IOI Oleochemicals GmbH, Germany). Tween[®] 80 (T80, polyoxyethylene sorbitan monooleate), Pluronic[®] F-68 (Poloxamer 188, P188), curcumin ($\geq 65\%$, HPLC, CRM), pentane (HPLC grade) and cinnamaldehyde (CA) were purchased from Sigma-Aldrich (Sigma-Aldrich, UK). Oxoid[™] phosphate-buffered saline (PBS) pH 7.4 tablets were obtained from Thermo Scientific (Sheffield, UK). Sunflower oil was purchased from a local supermarket, stored in a closed container at ambient temperature in the dark, and used without any further purification. Double distilled water from Milli-Q systems (Millipore, Watford, UK) was used during all sample preparation processes and characterization measurements.

2.2. Preparation of lipid particles

The aqueous dispersions of blank or curcumin-loaded SLNs and NLCs were prepared following a melt-emulsification-ultrasonication method that is fully described elsewhere (Sakellari et al., 2021a). The lipid melts (2.5% w/w) without or with curcumin (0.5% w/w of the lipid mass) were heated 5–10°C above the melting point of the solid lipid used (85°C for C888 and 70°C for P5) for 1 hr and were then combined with the aqueous surfactant solution (1.2% w/w T80 or P188). For the NLCs, 30% of the total lipid phase was substituted by

MCTs. The formed pre-emulsion was homogenized for 5 min using ultrasonication (Vibra-cell™ VC 505 Processor, Sonics & Materials, Inc., CT, USA), operating continuously at 750Watt and 20kHz, at a sonication amplitude of 95% of the total power. The crystalline particles were obtained by cooling the o/w emulsion using an ice bath to a temperature below the crystallization point of the lipid melts. Samples were stored at 4°C in the dark (since curcumin is photodegradable) until further analysis.

2.3. Particle size

Information about the particle size (Z-average) and polydispersity index (PDI) of the SLNs/NLCs was acquired with dynamic light scattering (DLS), using Zetasizer Nano ZS (Malvern Instruments, UK). All measurements were performed at a backscattering angle of 173° at 25°C, and samples were appropriately diluted with distilled water to avoid multiple scattering phenomena. The refractive indices were determined according to Sakellari et al. (2021a, 2022). All measurements were performed in triplicate, immediately after preparation and over time, and the average values with standard deviation (\pm S.D.) are presented. Representative size distributions of lipid particles were also obtained with laser diffraction (LD) using a Mastersizer 2000 (Malvern Instruments, UK), following a method that is described in detail below.

2.4. Interfacial tension

Dynamic interfacial oil/water tensions at 20°C were measured with a profile analysis tensiometer, using the pendant drop method (PAT-1M, Sinterface Technologies, Berlin, German). A drop of the SLN or NLC dispersions was suspended via a straight stainless-steel capillary (3mm outer diameter) in the sunflower oil phase contained in a quartz cuvette, with the cross-sectioned surface area remaining constant at 27mm². The measurements were performed until equilibrium was reached (the standard deviation of the last twenty measurements was smaller than 0.05mN/m). Density information was acquired using a densitometer (Densito, Mettler Toledo, US), at 20°C. All measurements were conducted in at least triplicate on three individually prepared samples.

2.5. Preparation of oil-in-water emulsions

Simple or Pickering o/w emulsions were prepared with 90% (w/w) aqueous phase containing either of the two surfactants at 1% w/w concentration, or any of the different (blank or curcumin-loaded) lipid nanoparticle systems, respectively, and 10% (w/w) sunflower oil phase. When cinnamaldehyde (0.3% w/w of the oil phase mass) was encapsulated within the oil droplets, the active and sunflower oil were stirred together for 1 h prior to the aqueous phase addition. During emulsification, which was performed employing ultrasonication under the same conditions as described above for a period of 30s, the samples were immersed in an ice bath to avoid shear-inducing heating and were later stored at 4°C until further analysis.

Emulsions that were thermally processed post-fabrication were heated at either 64 or 78°C (according to the melting events observed in the thermograms of the particle-stabilized emulsions) for 5, 20 or 60min (after the desired temperature was reached) using a hotplate under stirring, and were then cooled in an ice bath.

2.6. Droplet size measurements

Laser diffraction (LD) was utilized to obtain droplet size information, employing a Mastersizer 2000 (Malvern Instruments, UK) equipped with a Hydro SM manual small-volume sample dispersion unit. The stirrer speed was set at 1300rpm, and all samples were hand-mixed before analysis. The refractive index for sunflower oil was set at 1.47. All measurements were performed in triplicate on three individually prepared samples.

2.7. Thermal analysis

The thermal behavior of the SLNs and NLCs within the dispersion and emulsion systems was evaluated via Differential Scanning Calorimetry (DSC) using a Setaram μ DSC3 evo microcalorimeter (Setaram Instrumentation, France). The temperature cycle used ranged between 20 and 80°C at a heating rate of 1.2°C/min. The thermograms were obtained with the reference cell being filled with equal amount of distilled water. Data processing was carried out using the Calisto Processing software (Setaram Instrumentation, France), to obtain information regarding peak temperatures and melting enthalpies. The loss of crystalline matter for the emulsion systems was determined using information from the total melting enthalpies of the particles within an emulsion environment (ΔH_{em}^T) and those in an aqueous dispersion setting (ΔH_{dis}) and was expressed as a $\Delta H_{em}^T/\Delta H_{dis}$ ratio. The ΔH_{dis} and ΔH_{em}^T values were obtained from peak integration of the particle dispersion and particle-stabilized emulsion melting thermograms, respectively. All enthalpy values and thermograms reported, are normalized for the crystallizing material amount present in each sample. Specifically for the emulsion systems, each thermogram was normalized using the information of the respective SLN or NLC dispersion that was used for the emulsification. All measurements were performed in at least duplicate.

2.8. Encapsulation efficiency and loading capacity

The encapsulation efficiency (EE) and loading capacity (LC) of CRM-loaded particles and CA-loaded droplets was assessed by ultrafiltration using centrifugal ultrafiltration tubes (Amicon® Ultra-4 filter 10kDa cutoff, Millipore, Billerica, MA, USA). 1 mL of either the dispersion or emulsion systems was added to the upper chamber of the centrifugal tube and centrifuged at 2,400 rcf for 1 h at room temperature using a SIGMA 3K-30 centrifuge (SciQuip®, UK). The concentration of untrapped CRM or CA in the filtrate was subsequently determined by measuring the UV-Vis absorbance (Genova Bio Life Science Spectrophotometer, Jenway®, Cole-Palmer, UK) at 425 or

278 nm, respectively. Explicitly for CA, a solvent extraction protocol was followed prior to the absorbance measurements to eliminate any co-absorption interference at the specific wavelength. An aliquot of the filtrate was mixed with pentane at a 1:2 ratio, and the CA-rich pentane phase was then measured to determine the absorbance. The concentration of each model active was determined using calibration curves previously generated, with linearity studied for 0–6 µg/mL and linear regression value of $R^2 = 0.9995$ for CRM, and linearity of 0–28.7 µg/mL and $R^2 = 0.9915$ for CA. The EE and LC values were calculated using the following equations:

$$EE = \frac{W_i - W_u}{W_i} \times 100(\%) \quad (1)$$

$$LC = \frac{W_i - W_u}{W_{l.p.}} \times 100(\%) \quad (2)$$

where W_i is the amount of active that was initially used during the preparation of the aqueous lipid dispersions or emulsions, W_u is the amount of active measured in the filtrate, and $W_{l.p.}$ is the total amount of the lipid/oil components used in the systems.

2.9. In vitro release and co-release

In vitro release of curcumin, from curcumin-loaded lipid particle dispersions and particle-stabilized (Pickering) o/w emulsions was performed by diffusion through a dialysis membrane. A known amount of the particle dispersions or the Pickering emulsions was enclosed in a cellulose dialysis membrane (43 mm width, 14 kDa M.W. cutoff, Sigma-Aldrich Company Ltd., Dorset, UK), and the tubing was introduced in the *in vitro* release medium (130 g) consisting of phosphate buffer saline (PBS, pH 7.4) and 1.0% w/w Tween® 80. At pre-determined time intervals, 1 mL aliquots of the dissolution medium were collected and analyzed by UV-Vis spectrophotometry (Genova Bio Life Science Spectrophotometer, Jenway®, Cole-Palmer, UK). The *in vitro* release of cinnamaldehyde-loaded simple or Pickering emulsion droplets was assessed following the exact same protocol, with a slight modification at the absorbance measurement step, accordingly to what was previously described for the EE and LC determination. The absorbance was measured at 425 nm for CRM and at 278 nm for CA. The release measurements were performed using an Incu-Shake MIDI shaker incubator (Sciqip, UK) operating at 25 °C under constant shaking (180 rpm). The dissolution of CRM and CA solutions (at equal concentrations as those used in the dispersion/emulsion systems) prepared using the dissolution medium as solvent was also assessed. The dialysis membranes were soaked in the dissolution medium overnight, prior to usage. Sink conditions were maintained by replacing the sampled aliquots with equal volume of fresh media. The volume correction has been accounted for, in the reported cumulative release plots. The measurements were conducted in triplicate using independently prepared samples.

For the co-release assessments, the only adaptation in the above-described method was relevant to doubling the volume of aliquots withdrawn, to allow for sufficient quantification volume. For the stability assessments, the co-release measurements were performed immediately after preparation and after 1 month of storage at 4 °C.

2.10. Modeling of release data

The release data from the CRM-loaded lipid particles either in dispersion or emulsion settings were fitted into the mechanistic model described by Crank (1975), to gain further insight regarding the underlying release mechanism. The diffusion coefficient (D) was determined as follows:

$$\frac{Q_t}{Q_\infty} = 1 - \frac{6}{\pi^2} \sum_{n=1}^{\infty} \frac{1}{n^2} \exp\left(-\frac{Dn^2\pi^2t}{r^2}\right) \quad (3)$$

where Q_t is the mass of active released at time t , Q_∞ is the total mass of active released when the formulation is exhausted, n is the number of the term in the series, r is the particle radius (calculated using the Z-average), and D is the apparent diffusion coefficient of the active within the system.

Regarding the release of actives from within emulsion droplets, two limiting models have been previously described (Guy et al., 1982; Washington & Evans, 1995) and utilized in literature (Kurukji et al., 2016; Spyropoulos et al., 2020; Sakellari et al., 2021b). According to these, the release of the active is either primarily driven by diffusion through the oil droplet, or it is limited by the presence of an interfacial barrier around the emulsion droplet.

When the former is true, there is no interfacial barrier effect on the diffusion of the active through the oil core, and the release at long times can be approximated by:

$$\ln\left(1 - \frac{Q_t}{Q_\infty}\right) = \ln\left(\frac{6}{\pi^2}\right) - \frac{\pi^2 D}{r^2} t \quad (4)$$

which is the linear form of the following:

$$\frac{Q_t}{Q_\infty} = 1 - \frac{6}{\pi^2} \exp\left(-\frac{\pi^2 D}{r^2} t\right) \quad (5)$$

where symbols retain their previous meaning (Eq. (3)), but relevant to the emulsion droplets. For the emulsion radius (r), the $D_{3,2}$ data acquired from the LD measurements was used. Using Eq. (4) and plotting the $\ln(1 - Q_t/Q_\infty)$ against time will have a limiting slope of $(\pi^2 D/r^2)$, which can be used to calculate the diffusion coefficient D .

For the alternative model, where the active discharge is governed by the transfer across the interfacial barrier and the active is considered to be uniformly distributed within the emulsion droplet at all times, the following long-time approximation equation was used:

$$\frac{r^2}{3} \ln\left(1 - \frac{Q_t}{Q_\infty}\right) = -k_t t \quad (6)$$

which is the linear form of the following:

$$\frac{Q_t}{Q_\infty} = 1 - \exp\left(\frac{-3k_1 t}{r^2}\right) \quad (7)$$

where k_1 is the interfacial rate constant, with all other symbols retaining their meaning. Comparably to the previous model, plotting the natural logarithmic term on the left-hand side of Eq. (6) against time would provide with a straight line, the slope of which can be used to calculate k_1 .

The D values attained here were in the range of 10^{-11} , and thus significantly lower than those calculated using the Stokes–Einstein equation ($D = 1.3 \times 10^{-7} \text{ cm}^2 \text{ s}^{-1}$) for a small molecule diffusing through sunflower oil. If release was driven by diffusion, it would be expected that the estimated values would be close to that calculated by the Stokes–Einstein equation, but also close to one another, as the same oil phase was utilized in all formulations (Washington & Evans, 1995; Kurukji et al., 2016; Spyropoulos et al., 2020; Sakellari et al., 2021b). Therefore, the release should be primarily governed by transfer across the interfacial layer, rather than diffusion, and any k_1 differences should come as a result of interfaces with different barrier characteristics. The interfacial barrier-limiting model was further considered for the emulsion release behavior at longer times ($t \geq 30 \text{ min}$).

2.11. Statistical analysis

Samples were analyzed in at least triplicate, and averages are reported with standard deviation. Figures depict the calculated average value with error bars showing the standard deviation above and below the average. Comparison of means was conducted by ANOVA analysis followed by an all-pairwise multiple comparison test using the Student-Newman-Keuls Method (SigmaPlot 14.5). The differences were considered statistically significant when $p \leq 0.05$.

3. Results and discussion

3.1. Release from lipid particles

Recently, SLNs and NLCs were utilized as dual functional species, with the intent of simultaneously regulating the encapsulation/release of curcumin (used model hydrophobic active) and acting as Pickering emulsion stabilizers (Sakellari et al., 2022, 2023). Though the introduction of the loaded particles within the emulsion system was shown to accelerate the release rate compared to that recorded in a dispersion setting, both types of particles were still able to regulate the discharge of curcumin, with overall sustained release profiles being reported (~50% released over 7 days), while maintaining their Pickering stabilization capacity (Sakellari et al., 2023). Herein, the impact of modifying lipid particle formulation aspects, namely the type of solid lipid used and its combination with a liquid lipid, as well as the type of surfactant employed, on the release behavior in both an aqueous dispersion and an emulsion setting are explored.

3.1.1. Lipid particles in aqueous dispersions

Prior to introducing the lipid particles within the emulsion systems, their performance in aqueous dispersions was explored to establish how changes to the formulation parameters affect their release regulation ability (Figure 1). Based on previous investigations of the release performance of SLNs and NLCs fabricated with C888 as the solid lipid and MCTs as the liquid lipid, it was proposed that addition of MCTs results in the structural reorganisation of the particles' lipid matrix into a less ordered crystalline state, a phenomenon that in turn decreased the rate of curcumin release (Sakellari et al., 2023). Additionally, the release mechanism was described as diffusion-driven, due to both the overall slow release rate and high EE/LC values for either type of particles, and the low diffusion coefficients (D) as determined by the Crank model (Eq. (3)).

Delving further into the influence of modifying the lipid particles' composition, the high melting point solid lipid C888

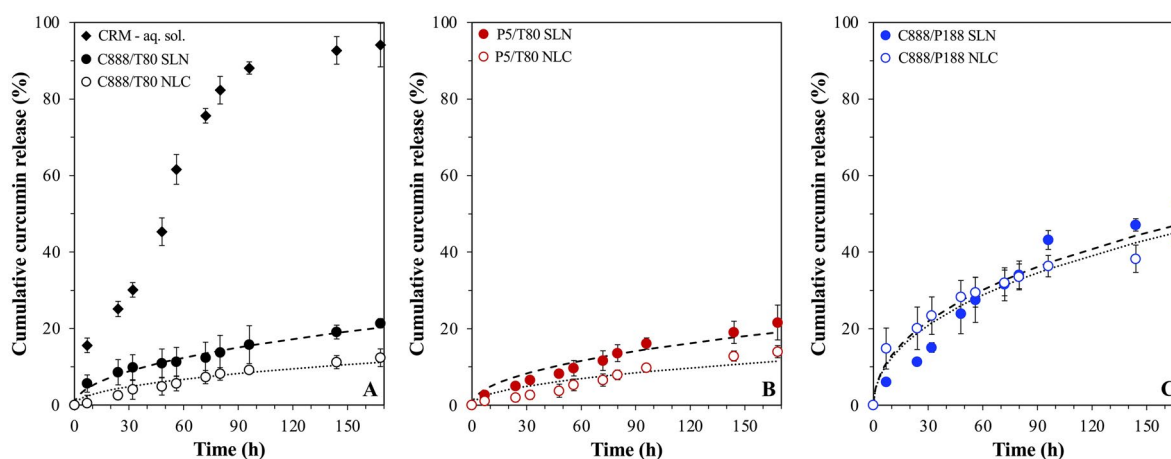


Figure 1. *In vitro* release profile of curcumin-loaded SLN and NLC dispersions formulated with either Tween® 80 (T80) as surfactant and different types of solid lipid (A) Compritol® 888 ATO (C888) and (B) Precirol® ATO 5 (P5), or different surface active species (C) Poloxamer 188 (P188) and C888 as solid lipid. NLCs were fabricated with Miglyol® 812 as the liquid lipid, at 30% w/w of the total lipid phase mass. The release profile from a curcumin solution obtained under the same conditions is also depicted (a). The *in vitro* release kinetic Crank model (Eq. (3)) fitting of curcumin for each SLN (dashed line) and NLC (dotted line) dispersion is also presented. Graph A has been previously shown in (Sakellari et al., 2023) and is provided here for comparison purposes.

was substituted by the lower melting point P5, keeping the rest of the formulation aspects unchanged, and the release performance of P5 SLNs and NLCs was investigated (Figure 1(B)). Compared to their C888 counterparts (Figure 1(A)), both lipid particle types demonstrated almost identical release profiles and very similar D values (Table 1). According to previously reported solubility studies (Sakellari et al., 2021a), C888 and P5 have comparable CRM solubility thresholds (0.6 and 0.7%, respectively), while their EE and LC values were the same ($99.9 \pm 0.0\%$ and $0.5 \pm 0.0\%$, respectively). Considering the above, it could be assumed that the localization of curcumin and/or internal arrangement of the lipid particles, for both the SLNs, but also the NLCs pairs were akin. Several studies have discussed the incapacity of the crystalline lipid structure of SLNs to host active molecules, and the subsequent expulsion/migration of the latter toward the surface of the particles (Jores et al., 2004; Kishore et al., 2012; Gordillo-Galeano et al., 2022). Correspondingly, addition of the liquid lipid component within the solid matrix has

been associated with solid/liquid phase separation, particularly at higher liquid lipid concentrations, and concentration-dependent creation of distinct lipid structures (Jenning et al., 2000; Jores et al., 2003; Sakellari et al., 2021a). With reference to the latter, it has been reported that once the solid lipids' solubility limit for the liquid component is exceeded, liquid oil nano-compartments can be formed within the matrix, or the liquid lipid can be concurrently expelled toward the surface (Jores et al., 2004, 2005). The formation of these compartments requires that sufficient space is available within the arrangement/packing of the crystalline element. Specifically for C888, when the lipid is crystallized at a cooling rate of $1^\circ\text{C}/\text{min}$, which is very close to the one used in this work ($1.2^\circ\text{C}/\text{min}$), the co-presence of two lamellae has been reported (Brubach et al., 2007), leading to matrix imperfections (Souto et al., 2006). Recently, Gordillo-Galeano et al. (2022) described the stages of active (paraben) exclusion as the lipid matrix crystallizes, toward the MCTs-rich surface of trimyristin NLCs, or in-between the trimyristin crystals and the surfactant (P188) layer in SLNs. In the present study, both C888 and P5 are mixtures of variable triacylglycerols; the former of slightly longer alkyl chains, while the latter of more varied composition (behenic acid and palmitic/stearic acid esters, respectively). Additionally, in both types of NLCs, the prospect of the presence of polymorphs characterized by lower packing densities has been previously discussed (Figure 2(A and B)) (Sakellari et al., 2021a), thereby not utterly excluding the possibility of MCTs compartment formation within the NLCs' structure (Macridachis-González et al., 2020; Bertoni et al., 2021). However, taking into account that MCTs was used at a 30% w/w concentration of the total lipid phase, which was likely exceeding the solubility limits of either solid lipids for MCTs, it was expected that the bulk of the liquid lipid component would be contained near the surface of the particles (Jores et al., 2004, 2005). Consequently, given the

Table 1. Diffusion coefficient (D) and coefficient of determination (R^2) describing the fitting into the Crank model (Eq. (3)) of the curcumin release data from lipid particles within dispersion and emulsion systems. Identical lowercase letters indicate no significant differences between samples.

Lipid particle setting	Lipid formulation	$D \times 10^{-20}$ (cm^2s^{-1})	R^2
Dispersions	C888/T80 SLN	45.1 ± 7.9^a	0.98
	C888/T80 NLC	12.1 ± 1.4^a	0.97
	P5/T80 SLN	45.0 ± 3.7^a	0.96
	P5/T80 NLC	6.6 ± 1.2^a	0.95
	C888/P188 SLN	214 ± 34.5^b	0.94
Emulsions	C888/P188 NLC	178 ± 23.1^b	0.98
	C888/T80 SLN	213 ± 23.2^b	0.94
	C888/T80 NLC	177 ± 25.4^b	0.97
	P5/T80 SLN	546 ± 45.1^c	0.96
	P5/T80 NLC	171 ± 45.8^b	0.98
	C888/P188 SLN	278 ± 39.0^b	0.99
	C888/P188 NLC	310 ± 51.0^b	0.99

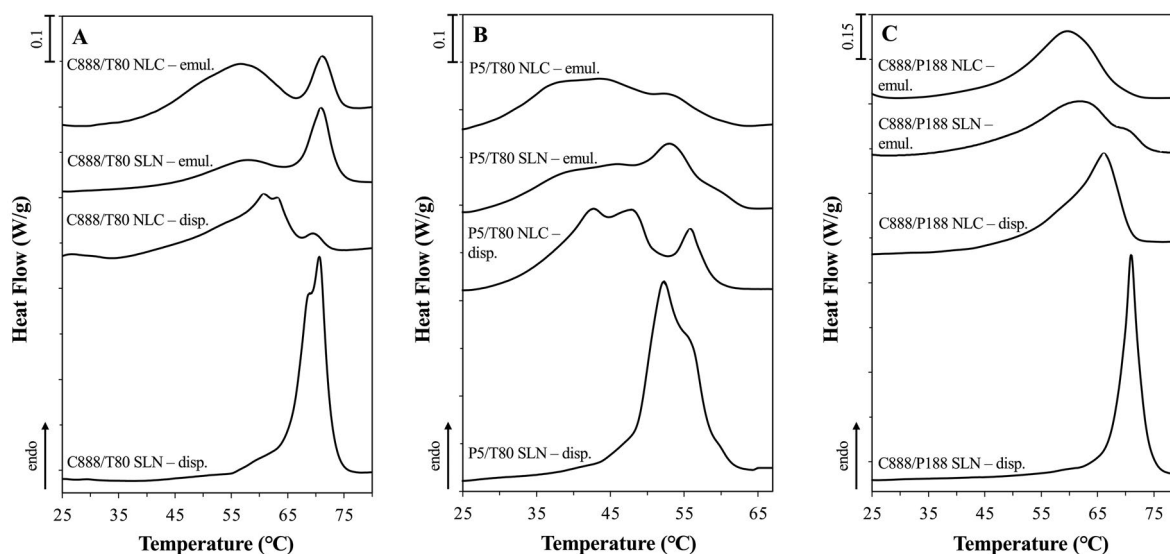


Figure 2. DSC melting thermograms of SLN and NLC dispersions and their respective Pickering emulsions, for lipid particles formulated with either Tween[®] 80 (T80) as surfactant and different types of solid lipid (A) Compritrol[®] 888 ATO (C888) and (B) Precirol[®] ATO 5 (P5), or different surface active species (C) Poloxamer 188 (P188) and C888 as solid lipid. NLCs were fabricated with Miglyol[®] 812 as the liquid lipid, at 30% w/w of the total lipid phase mass. The curves were normalized for the amount of solid matter present in each sample and shifted along the ordinate for better visualization. Graph A has been previously shown in literature (Sakellari et al., 2022, 2023) and is provided here for comparison purposes.

solubility constrains imposed by the solid lipid crystallization, it could be hypothesized that CRM would be preferentially located within the MCTs phase (NLCs) or near the surface of the particles (SLNs), at least when it comes to its highest proportion (Anantachaisilp et al., 2010; Shah et al., 2012; Gordillo-Galeano et al., 2022).

The next parameter assessed was the effect of lipid particle formation in the presence of different surface active species, on the CRM release, with both SLNs and NLCs fabricated with P188 as surfactant and C888 as the solid lipid (Figure 1(C)). Compared to their T80 counterparts, both P188 particle types exhibited faster release. Furthermore, there was almost no difference between the C888/P188 SLN and NLC formulations, as opposed to the slower NLC release recorded for the particles fabricated with T80 for either type of solid lipid. The *D* values calculated for these systems (Table 1), although higher than the particles formed with T80, were still significantly lower than values reported in literature for curcumin-loaded SLNs fabricated with stearic acid as the lipid phase and P188 as surfactant (Tiyaboonchai et al., 2007; Sakellari et al., 2021b). The Crank model described well the diffusion-driven release, despite the slightly less ideal fitting for C888/P188 SLNs, which could be explained by the initially predicted faster release by the model, compared to the experimentally collected data. Taking into consideration that there were only very small particle size differences (Table 2), and the EE/LC values remained the same in all particle types (Sakellari et al., 2021a), it could be suggested that the discrepancies in the release behavior were driven by the surfactant substitution. Based on the melting behavior of the C888/P188 lipid particles where a diminished degree of polymorphism was observed (Figure 2(C)), and previous investigations regarding the compatibility between the lipid matrix components (Sakellari et al., 2021a), T80 appeared to participate at a greater extent (than P188) within the crystalline network (close to the particle surface). Therefore, it could be also postulated that the co-existence of C888/T80 in SLNs or MCTs/T80 in the case of NLCs at the edge of the particles' structure and near the particles' surface is posing an additional barrier for CRM to cross, possibly due to the creation of a favorable hydrophobic environment compared to the dissolution medium. Contrary to the potentially denser packing arrangement provided by the smaller T80 molecules, the larger molecular sized P188 molecules could not provide an as tightly packed interface, which together with their limited crystalline network participation, due to their more hydrophilic character, could not permit a strong retention of CRM, in both the P188-decorated SLNs and NLCs (Badawi et al., 2020).

Table 2. Z-average and polydispersity index (PDI) of different SLN and NLC formulations measured after preparation.

Formulation	Z-average (nm)	PDI
C888/T80 SLN	165.1 ± 2.7	0.20 ± 0.02
C888/T80 NLC	163.2 ± 3.8	0.12 ± 0.01
P5/T80 SLN	176.0 ± 9.6	0.28 ± 0.04
P5/T80 NLC	134.4 ± 7.1	0.14 ± 0.04
C888/P188 SLN	139.7 ± 1.9	0.20 ± 0.01
C888/P188 NLC	133.7 ± 2.1	0.18 ± 0.02

With respect to the sustained release rate from all six lipid particle types (<50% CRM released cumulatively in 7 days), similar trends have been previously reported for SLNs and NLCs encapsulating hydrophobic moieties (Ugazio et al., 2002; Hu et al., 2004; Venkateswarlu & Manjunath, 2004; Luo et al., 2006). Such sustained release profiles were usually ascribed to hindered diffusion of the active molecules through the highly ordered crystalline arrangement of the lipid particles, though active partition coefficients and solubility constraints could also contribute to the stunted release percentages and lengthy experimental times (Bunjes, 2010; Noack et al., 2012; Salminen et al., 2014, 2016). Herein, the dissolution medium was selected based on two criteria; firstly, it was prerequisite to have sufficient solubilization capacity for the amount of active present in the particle dispersions during the release studies (sink conditions), and secondly based on previously reported literature (Shahani & Panyam, 2011; Zhao et al., 2022b), and its use in similar systems, it was anticipated that it would not impact on the lipid particles' integrity over the timescales of the measurement, to ensure that the effect of the formulation aspects was adequately represented. However, it should also be noted that the selection of a solvent for which CRM has a higher affinity compared to the selected lipids, and hence would result in lower partition coefficient (Zur Mühlen et al., 1998; Rosenblatt & Bunjes, 2009), and/or higher solubility thresholds, could have also potentially led to much faster release rates. Therefore, the results presented here in terms of the release profiles, but also with regard to the diffusion coefficients, should only be approached as a relative measure of the influence of formulation parameter changes.

3.1.2. Lipid particles in emulsions

The dual role of both SLNs and NLCs to act as Pickering stabilizers and in tandem as release regulators of CRM has been previously shown, using particles fabricated with C888 and T80 (Sakellari et al., 2022, 2023). Particular focus was placed on the lipid particle and particle-stabilized emulsion properties that can have an effect on the release behavior (e.g. solid-to-liquid lipid mass ratio of the lipid particles), and the underlying mechanism that drives said release. It was suggested that the CRM discharge from particle-loaded Pickering emulsions is the composite of the release from particles remaining dispersed in the continuous aqueous phase, and particles positioned at the oil-water droplet interface (Sakellari et al., 2023). The increased release rate from emulsions, compared to that from particle dispersions, was attributed to partial migration of particle-entrapped curcumin to the oil phase (droplets) as well as to a limited loss of crystalline matter from the particles (again into the emulsion droplets). Therefore, before probing deeper into the release performance of lipid particles with modified formulation parameters, namely type of solid lipid and surfactant, physical characteristics of both the particle dispersions and the respective particle-stabilized emulsions were scrutinized. This was performed to gain further insight into the microstructural properties of the formed systems, particularly in terms of their Pickering behavior.

Among these was the interfacial tension reduction capacity of the particles (Figure 3), based on which information regarding the interfacial decoration of the particles could be extracted. It was observed that both P5 fabricated particle types had identical interfacial tension reduction ability with an equilibrium value of 6.3 mN/m (Figure 3(B)), which was similar as that recorded for the C888 NLCs (Figure 3(A)), but higher than the C888 SLNs. Considering that all T80-formed particles had similar sizes, and an equal amount of surfactant was employed during their fabrication, this disparity could be attributed to differences in the lipid composition of the particles affecting the arrangement and packing density of surfactant molecules at their surface. Particles prepared with P188 as the surfactant demonstrated considerably higher equilibrium interfacial tension values; 15.3 and 14.3 mN/m for the SLNs and NLCs, respectively (Figure 3(C)). This could be due to differences in the molecular size of the two surfactants, which in turn could be resulting in different packing arrangements at the particles' surface. T80 seemed to

instigate a higher interfacial tension reduction compared to P188, possibly owing to a higher and more tightly packed interfacial presence, caused by its smaller molecular size, as supported by the trends of both aqueous surfactant solution curves (Zafeiri et al., 2017a). The effect of the surfactant molecular size was also reflected in the obtained emulsion droplet sizes. Regardless of the type of solid lipid used or type of lipid particle (SLN/NLC) created, particles fabricated with T80 exhibited almost identical droplet size distributions (Figure 4(A and B)), while P188 particles formed droplets that were an order of magnitude larger (Figure 4(C)).

The loss of crystalline matter once the particles were introduced within the emulsion systems was also explored, as this has been suggested as a factor impacting their release behavior. According to Figure 5, there was a greater loss of crystalline material for the P5/T80 SLNs/NLCs compared to the C888 containing particles. As it has already been suggested in literature (Samtlebe et al., 2012; Zafeiri et al., 2017b; Sakellari et al., 2023), the type of lipid source used can play

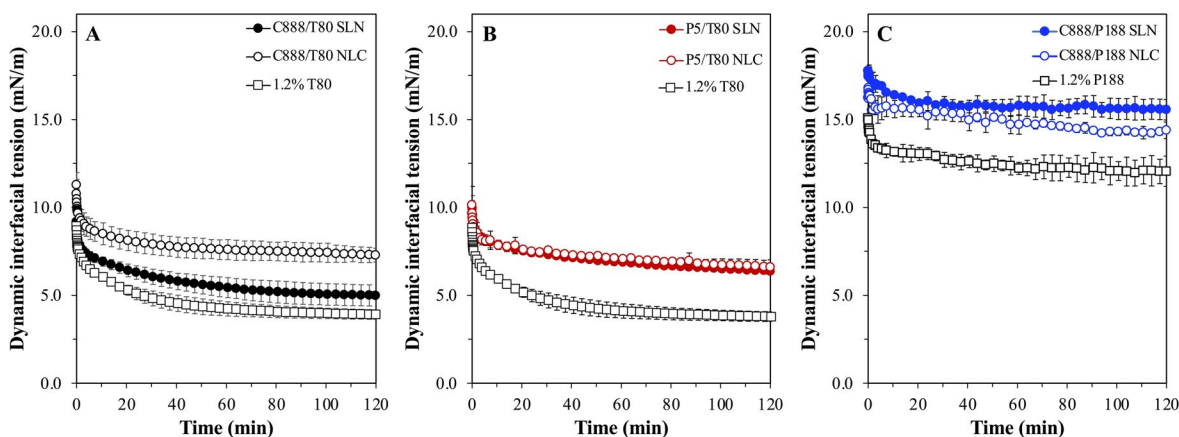


Figure 3. Dynamic interfacial tension of aqueous dispersions of SLN and NLC formulations prepared with either Tween® 80 (T80) as surfactant and different types of solid lipid (A) Compritol® 888 ATO (C888) and (B) Precirol® ATO 5 (P5), or different surface active species (C) Poloxamer 188 (P188) and C888 as solid lipid. NLCs were fabricated with Miglyol® 812 as the liquid lipid, at 30% w/w of the total lipid phase mass. The curves of pure T80 and P188 solutions with similar concentration (1.2% w/w) as of those used for the dispersions are also presented for comparison. Data points are the average of three measurements and error bars represent the standard deviation. Graph A has been previously shown in (Sakellari et al., 2022) and is provided here for comparison purposes.

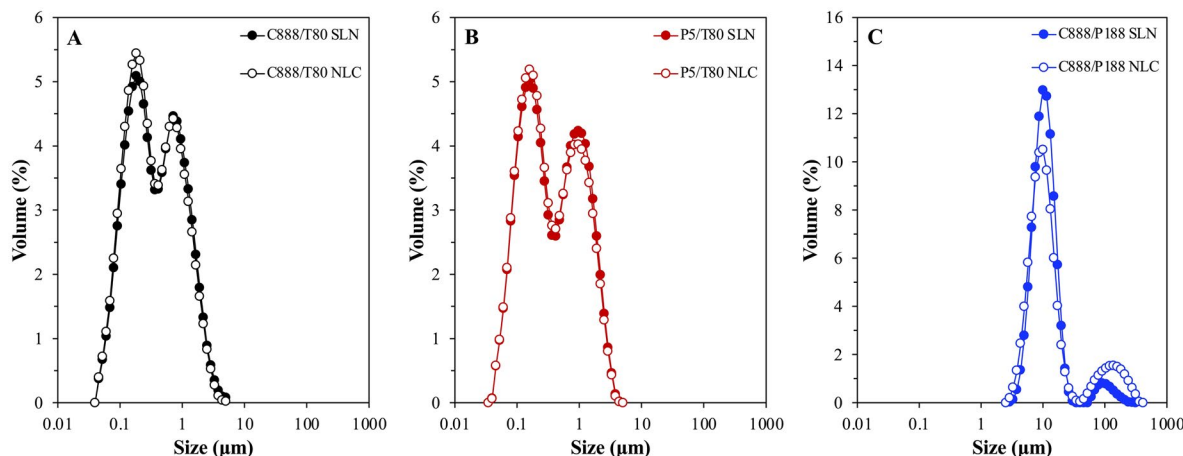


Figure 4. Droplet size distribution of SLN- and NLC-stabilized emulsions, with lipid particles formulated with either Tween® 80 (T80) as surfactant and different types of solid lipid (A) Compritol® 888 ATO (C888) and (B) Precirol® ATO 5 (P5), or different surface active species (C) Poloxamer 188 (P188) and C888 as solid lipid. NLCs were fabricated with Miglyol® 812 as the liquid lipid, at 30% w/w of the total lipid phase mass. Graph A has been previously shown in (Sakellari et al., 2022) and is provided here for comparison purposes.

a crucial role in lipid mass transfer phenomena, with surfactant micelles facilitating the transfer of oil molecules from the emulsion droplets to the particles' lipid core. Such occurrences could either be directly related to particles adsorbed at the emulsion interface or even particles remaining free in the continuous phase. In this instance, it appeared that the potentially higher compatibility of P5 (glyceryl palmitostearate) and sunflower oil (containing triglycerides of palmitic and stearic acids), due to their closer chemical composition compared to that between C888 and sunflower oil, could be further aiding dissolution (Jamieson & Baughman, 1922; Sakellari et al., 2021a). On the contrary, emulsion formation did not cause any losses of crystalline matter for the C888/P188 particles, possibly owing to the improved protection provided by the P188 molecules over such incidents. As

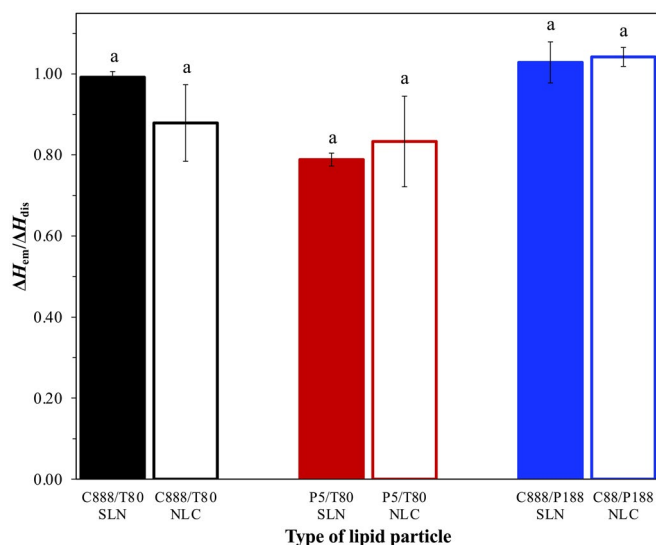


Figure 5. Ratio of the melting enthalpies of the particles within an emulsion environment and those in a lipid particle dispersion setting ($\Delta H_{em}^T/\Delta H_{dis}^T$), representing the amount of crystalline material remaining within the emulsions stabilized by different types of lipid particles. Identical lowercase letters indicate no significant differences between samples.

mentioned earlier, besides the type of lipid source, another aspect affecting this event was the formation and presence of surfactant micelles within the continuous phase (McClements et al., 1993a,b; McClements & Dungan, 1993; Weiss & McClements, 2000); in this instance, introduced to the system from the continuous phase of the particle dispersions (remnant unadsorbed surfactant). A previous study exploring the impact of removal of excess unadsorbed surfactant from the continuous phase of the lipid particle dispersions (prior to their use during emulsification) on crystalline matters loses, revealed that although there was no difference for dialyzed and undialysed SLNs, when it came to NLCs, dialysis helped decrease mass transfer phenomena following the addition of the oil phase (Sakellari et al., 2023). In this work, the aqueous P188 concentration even before addition to the pre-emulsion used for the particle dispersion production, was a lot lower than its critical micelle concentration (CMC, 17.9 mM) (Alexandridis et al., 1994). Therefore, the lack of micelles present in the systems to facilitate any mass transfer, in combination with the usage of a lipid (C888) with very low aqueous solubility (Samtlebe et al., 2012) has led to no losses compared to the already minimal crystalline matter reduction reported for the C888/T80 particles. Lastly, the fewer particle/oil contact points should be accounted, as the proportion of C888/P188 particles required to cover the oil droplet surface area was a lot less than that of the C888/T80 particles, due to the significantly larger emulsion droplet sizes produced with the former, as primarily shown for the NLCs (Figure 4).

With regard to their release regulation ability, both particle types prepared with P5 exhibited faster release compared to the particles fabricated with C888, while P5 NLCs release slightly less of their content than the P5 SLNs (Figure 6(A and B)). The greater loss of crystalline matter in the P5/T80 SLNs/NLCs (Figure 5) could account for the higher release rate, particularly in the first 48 h of the experiment. Conversely, the CRM release rate from both P188-formed SLNs and NLCs at the emulsion interface was only marginally higher to that

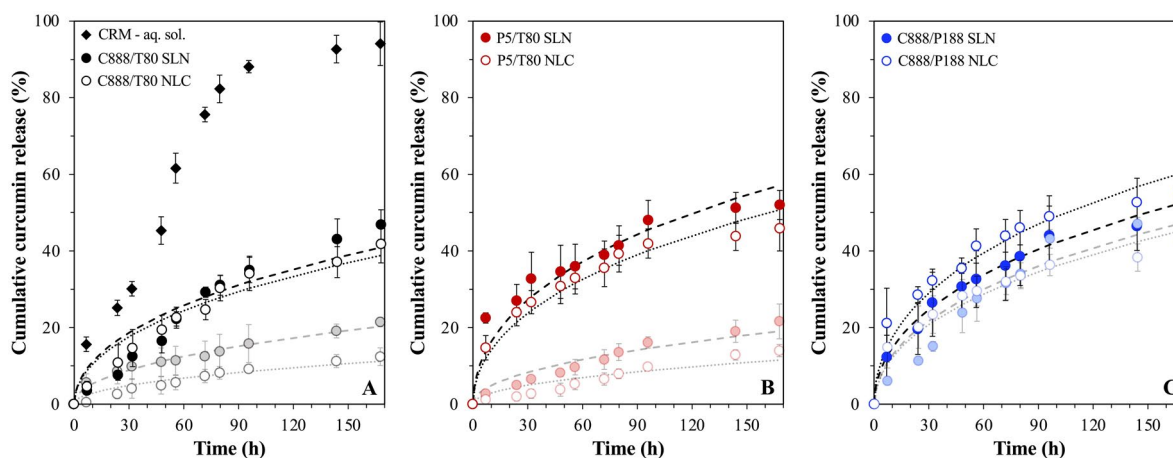


Figure 6. *In vitro* release profile of curcumin-loaded SLN- and NLC-stabilized emulsions formulated with either Tween® 80 (T80) as surfactant and different types of solid lipid (A) Compritol® 888 ATO (C888) and (B) Precirol® ATO 5 (P5), or different surface active species (C) Poloxamer 188 (P188) and C888 as solid lipid. NLCs were fabricated with Miglyol® 812 as the liquid lipid, at 30% w/w of the total lipid phase mass. The *in vitro* release kinetic Crank model (Eq. (3)) fitting of curcumin for each emulsion system stabilized by SLNs (dashed line) or NLCs (dotted line) is also presented. The release profile from a curcumin solution obtained under the same conditions (a) and that of the particles within the dispersion systems are also depicted in each respective graph. Graph A has been previously shown in the literature (Sakellari et al., 2023) and is provided here for comparison purposes.

exhibited by the particles in an aqueous dispersion setting (Figure 6(C)). The absence of any micelles available to facilitate the dissolution of solid matter and thereby release of any CRM associated with it, as well as the higher percentage of unadsorbed C888/P188 particles in the continuous phase (due to the lower number required to cover the smaller droplet surface area), were hypothesized to be the reasons for this lack of release profile changes. The calculated diffusion coefficient values were in the same order of magnitude for all particle-stabilized emulsions (Table 1), with only exception the P5/T80 SLNs that were characterized by a significantly higher D value, which aligns well with the fact that this was the particle type with the higher loss of crystalline matter. The EE and LC remained the same as for the dispersions ($99.9 \pm 0.0\%$ and $0.5 \pm 0.0\%$, respectively).

3.2. Release from lipid particle-stabilized emulsion droplets

Within this work, apart from their active carrying and release regulation ability, lipid particles acted also in tandem as Pickering emulsion stabilizers. The latter functionality contributes to two main aspects, with lipid particle-laden interfaces: (i) promoting/ensuring droplet stabilization; and (ii) acting as a barrier/regulator for the release of a secondary active encapsulated within the emulsion droplets. There are two rate-limiting steps relevant to the release of an active from within emulsion droplets; active diffusion within the oil droplet and toward the interface, and active transfer across the interfacial barrier (Washington & Evans, 1995; Kurukji et al., 2016; Spyropoulos et al., 2020; Sakellari et al., 2021b). For the systems studied here, it was shown (see section 2.10) that release was governed by the interfacial transfer of the active and thus the formulation properties of the lipid particles formulated here were expected to have an impact on this interfacial barrier. In order to test this hypothesis, a range of SLNs and NLCs (investigated earlier for their curcumin (primary model active) discharge regulation), were utilized (in this case) as blank colloidal species

providing Pickering stabilization to emulsion droplets loaded with cinnamaldehyde, used as a (secondary) model hydrophobic active.

3.2.1. The effect of lipid particle formulation

For the purpose of establishing a reference for the impact of the particles' interfacial presence on both the droplets' active carrying and release capacity, simple emulsions fabricated with either of the two surface active species used for lipid particle preparation (T80 or P188) were also studied. Compared to a cinnamaldehyde (CA) solution, confining the active within the emulsion droplets appeared to slow down the release rate to a certain degree, with full discharge achieved within 100 min for the former (CA solution) and a delay (to full release) of 50 and 150 min recorded for the P188 and T80 stabilized emulsions, respectively (Figure 7(A)). Droplet size characteristics and EE/LC values were also determined, with both emulsions showing bimodal size distributions with a main peak at around $1 \mu\text{m}$ and a smaller one at $\sim 0.25 \mu\text{m}$ (Figure 7(B)), and no significant differences in the attained EE and LC values (approximately 83% and $7.6 \times 10^{-3}\%$, respectively) (Table 3). In contrast, the interfacial presence of the lipid particulates seemed to slow down the cinnamaldehyde release rate and overall percentage discharged. Approximately, 75% release was reached at 280 min for both C888/T80 and P5/T80 particles, and 40% was released at the same timescale for the C888/P188 counterparts, while almost identical profiles were obtained for SLNs and NLCs with the same formulation characteristics (Figure 8). In terms of the capacity of the particles to improve the amount of active remaining contained within the droplets, the EE and LC values were in the same range as for the simple emulsions (Table 3). This suggested that the active retention within the droplets was predominantly governed by the characteristics of the oil phase, rather than their interfacial decoration.

Even though o/w emulsions represent a suitable and adaptable platform for the encapsulation and delivery of poorly water-soluble actives, the absence of a more robust barrier at the droplet interface can lead to burst release and

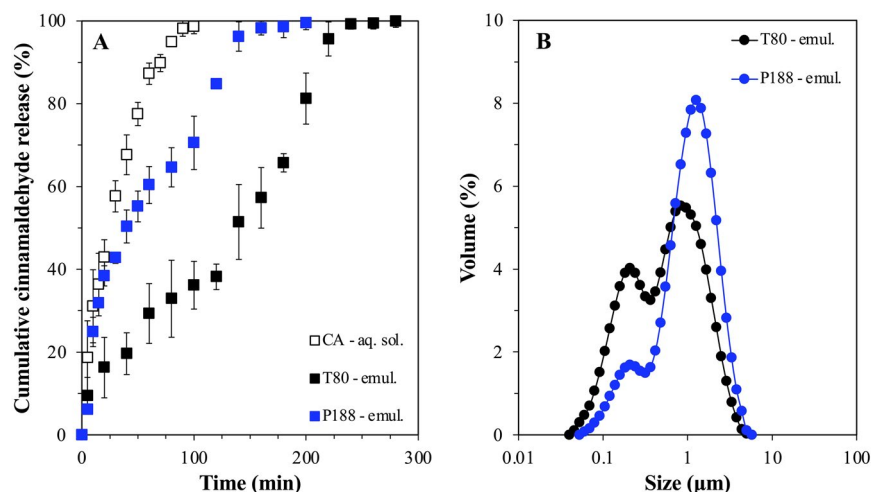


Figure 7. *In vitro* release profile of cinnamaldehyde-loaded emulsions stabilized with either Tween® 80 (T80) or Poloxamer 188 (P188) (a), droplet size distribution of the same systems (B). The release profile from a CA solution obtained under the same conditions is also depicted (a).

active expulsion overtime (Simovic & Prestidge, 2007; Frelichowska et al., 2009a,b; Dickinson, 2010). Herein, it was shown that differences in the interfacial composition, from surfactant molecules to lipid particles, and even more specifically changes in the structure of the particles themselves, did in fact alter the release kinetics. In literature, complete release from simple emulsions has been shown to occur over varying timescales ranging from a couple of minutes for small hydrophobic solutes such as chlorpromazine from soya oil droplets stabilized with P188 (Washington & Evans, 1995), to a couple of hours for the release of dibutylphthalate from bare polydimethylsiloxane droplets (Prestidge & Simovic, 2006). This aligns well with the data reported here, as any small difference could be related to disparities in the droplet sizes variations in the partition coefficient values between the used active, oil phase and dissolution medium, and/or altered release measurement methods. Concerning the effect of the particle addition, preliminary studies revealed that the incorporation of cinnamaldehyde did not alter the physical properties of the formed Pickering emulsions. Therefore, required information regarding the droplet sizes to estimate

the interfacial rate constant (k_1) values (Eq. (6)), was used according to Figure 4. The k_1 values estimated in this work were in the range of $10^{-15} \text{ cm}^2 \text{ s}^{-1}$ for the emulsions stabilized by T80-formed particles and almost three orders of magnitude larger for the C888/P188 SLNs/NLCs-stabilized emulsions (Table 3). Similar values to the C888/P188 particle-stabilized emulsions have been described for dimethyl phthalate releasing from emulsions stabilized with SLNs prepared using whey protein isolate ($3.1 \times 10^{-12} \text{ cm}^2 \text{ s}^{-1}$) (Sakellari et al., 2021b), as well as emulsions stabilized by surfactants with Pickering-like characteristics (Spyropoulos et al., 2020). On the contrary, emulsions stabilized with T80 particles gave values akin to previously reported data for emulsions stabilized by silica particles (Prestidge & Simovic, 2006; Simovic & Prestidge, 2007) and protein/polysaccharide co-precipitates (Kurukji et al., 2016). Such deviations could be ascribed to disparities in the active partition coefficient and dissolution medium solubility values amongst the various studies. However, despite the much greater k_1 values for the C888/P188 SLNs/NLCs, the experimentally recorded release rate for CA was much slower compared to that of their C888/T80 and P5/T80 counterparts. This could be due to the fact that the interfacial area of the C888/P188 SLNs/NLCs-stabilized emulsions is much lower (almost 10-times higher droplet size) compared to the C888/T80 or P5/T80-stabilized droplets, which could be also contributing to the worse fitting of the interfacial-barrier model (Table 3).

Overall, both SLNs and NLCs were shown to act as effective interfacial barriers against the burst release of a model hydrophobic active enclosed in the lipid particle-stabilized emulsion droplets. What is more, it was demonstrated that lipid particle characteristics (in this case, the type of surfactant used during particle fabrication) can be significant factors in terms of active release across a lipid particle-laden interface. Thus, such particle characteristics could be controlled at the particle fabrication stage, in order to provide interfacial barriers with a specific release performance (Deshmukh et al., 2015; Ming et al., 2022). The same principle should potentially also apply to manipulating particle size, a

Table 3. Encapsulation efficiency (EE), loading capacity (LC), interfacial rate constant coefficient (k_1), and coefficient of determination (R^2) describing the model fitting for the interfacial barrier-limiting model of the cinnamaldehyde release data from emulsion systems. Identical lowercase letters indicate no significant differences between samples.

Formulation	EE (%)	LC $\times 10^{-3}$ (%)	$k_1 \times 10^{-15}$ ($\text{cm}^2 \text{ s}^{-1}$)	R^2
T80	84.2 \pm 1.0 ^a	7.8 \pm 0.0 ^a	–	–
P188	83.3 \pm 2.8 ^a	7.6 \pm 0.0 ^b	–	–
C888/T80 SLN	80.7 \pm 1.1 ^a	7.7 \pm 0.0 ^c	3.9 \pm 1.5 ^a	0.98
C888/T80 NLC	88.1 \pm 3.8 ^a	8.6 \pm 0.0 ^d	2.6 \pm 0.4 ^a	0.99
P5/T80 SLN	82.9 \pm 2.5 ^a	7.7 \pm 0.0 ^e	2.8 \pm 0.6 ^a	0.99
P5/T80 NLC	83.5 \pm 3.3 ^a	7.9 \pm 0.0 ^f	2.4 \pm 0.5 ^a	0.99
C888/P188 SLN	84.4 \pm 1.4 ^a	8.1 \pm 0.0 ^g	1900 \pm 45 ^b	0.94
C888/P188 NLC	88.0 \pm 2.1 ^a	8.1 \pm 0.0 ^h	1700 \pm 53 ^c	0.94
C888/T80 SLN – 64 °C 5 min	80.7 \pm 0.9 ^a	7.7 \pm 0.0 ^c	1.4 \pm 0.7 ^a	0.98
C888/T80 SLN – 64 °C 20 min	80.9 \pm 0.8 ^a	7.7 \pm 0.0 ^c	1.4 \pm 0.9 ^a	0.96
C888/T80 SLN – 64 °C 60 min	81.0 \pm 1.0 ^a	7.7 \pm 0.0 ^c	2.2 \pm 0.5 ^a	0.94

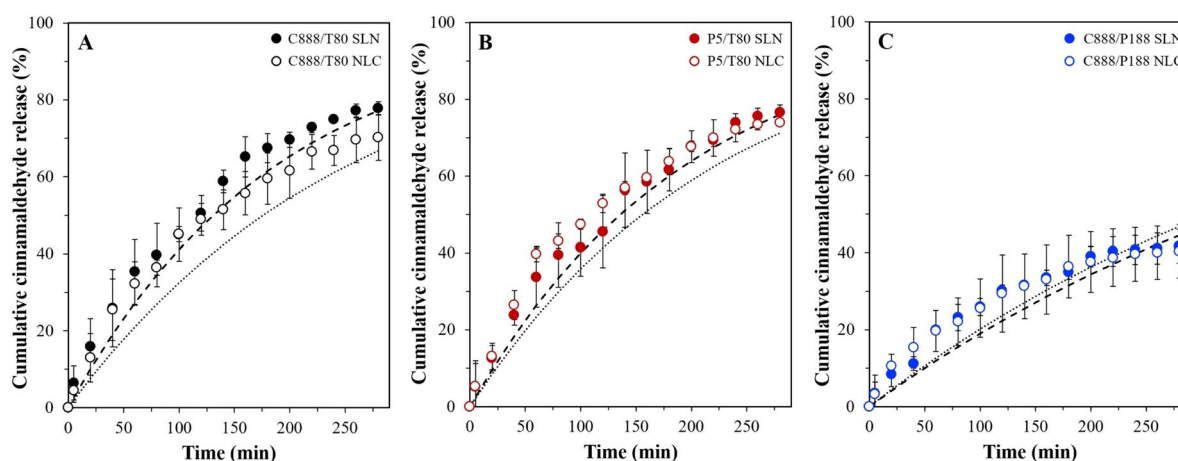


Figure 8. *In vitro* release profile of cinnamaldehyde-loaded emulsions stabilized by SLNs and NLCs formulated with either Tween® 80 (T80) as surfactant and different types of solid lipid (A) Compritol® 888 ATO (C888) and (B) Precirol® ATO 5 (P5), or different surface active species (C) Poloxamer 188 (P188) and C888 as solid lipid. NLCs were fabricated with Miglyol® 812 as the liquid lipid, at 30% w/w of the total lipid phase mass. The interfacial barrier-limiting model (Eq. (6)) fits to the data for the release of cinnamaldehyde from the SLN- (dashed line) and NLC- (dotted line) stabilized emulsions are also presented.

feature that was not specifically investigated here and was practically kept unchanged across the studied SLN/NLC particles.

3.2.2. The effect of interfacial sintering

To further evaluate the plausibility of controlling the active discharge from within the o/w emulsion droplets by manipulating the lipid particle-laden interfacial architecture, the newly prepared Pickering emulsions were subjected (post-production) to thermal processing. The occurrence of solid bridge formation between neighboring fat crystals that are driven by mutual adhesion, also known as sintering, has been previously discussed in literature as a means of controlling the strength of a lipid-based structure and the texture of the resulting products (Johansson & Bergenst ahl, 1995). Thermal sintering has been widely utilized as a preparation method for colloidosomes, thereby creating a robust layer at the oil/water interface that can provide not only improved protection against destabilization phenomena, but also create microcapsules suitable for carrying and delivering active molecules (Dinsmore et al., 2002; Yow & Routh, 2009). To this end, C888/T80 SLN-stabilized emulsions were heated (post-production) at either 64°C or 78°C under mild stirring for varying times, and changes in their physical properties and (release) performance were studied. According to earlier work using the particle-stabilized emulsions (Sakellari et al., 2023), the two peaks at ~60°C and 70°C observed in their melting thermograms were ascribed to either particles associated with the emulsion interface (adsorbed) or particles remaining free in the continuous phase (unadsorbed), respectively. Therefore, the temperatures selected for this proof-of-concept sintering assessment were based on said melting events, presented in Figure 9(A).

Heating of the SLN-stabilized emulsions (post-production) at 64°C for increasing timescales (5, 20 and 60 min) caused a statistically significant loss of crystalline matter compared to the untreated system, although the loss was overall minimal

with all systems maintaining >90% of their initial solid content intact post thermal processing (Figure 9(B)). When the emulsions were heated at the highest temperature (78°C), the melting profile of the system in terms of the relative intensity of the peaks appeared altered, with the peak at 62°C being more pronounced than that at 70°C, suggesting a decrease in the proportion of particles remaining unadsorbed in the continuous phase. Following the extended heating at 78°C, partial phase separation was observed with a visible oil layer formed at the top of the emulsion. An increase in droplet size was also recorded here, possibly due to droplet and/or particle aggregation events induced by the complete melting of the lipid particles both at the droplet interface and within the continuous phase (Figure 10(A)). However, it is not clear whether shorter periods of exposure at this temperature would yield similarly compromised formulations. It is worth noting that despite the slight loss to their crystalline integrity, SLN-stabilized emulsions heated at 64°C were able to maintain an unchanged droplet size distribution regardless of the duration of the thermal treatment.

In terms of release performance, emulsion that were thermally processed at 64°C displayed a more sustained release profile (compared to their untreated predecessor) with no differences observed between them, and around 50% of CA being released within 240 min, as opposed to the 75% achieved by their parent (non-heated) formulation (Figure 10(B)). Fitting of the interfacial barrier-limiting model gave k_1 values lower than for the unprocessed emulsion (Table 3). The release performance of samples heated at 78°C was not further assessed due to the oil phase separation and discrepancies that this would cause to the calculation of the percentage of active discharging from the remaining physically intact droplets. In a study by Yow & Routh (2009), the formation of colloidosomes from colloidal poly(styrene-co-butyl acrylate) particles via sintering at varying temperatures and durations, was examined in relation to the release of a model active (fluorescein). It was shown that manipulation of the

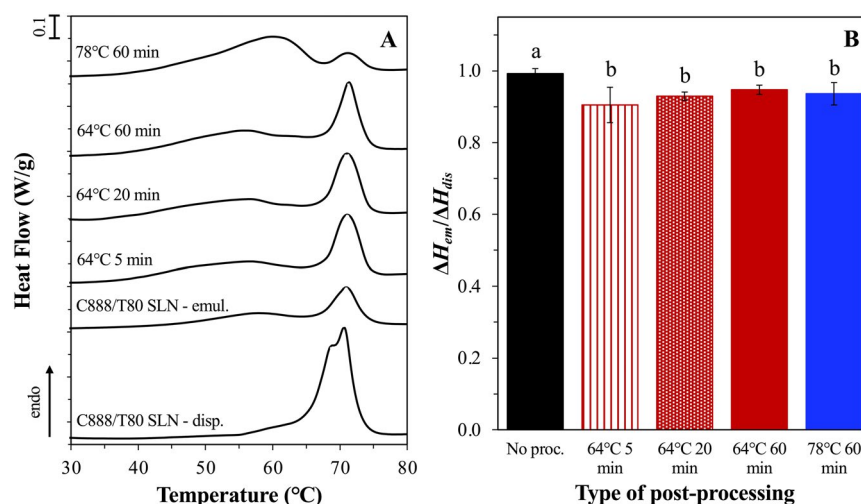


Figure 9. DSC melting thermograms of C888/T80 SLN-stabilized emulsions before and after sintering at 64 and 78°C for varying durations (a). The curves were normalized for the amount of solid matter present in each sample and shifted along the ordinate for better visualization. The melting curve of the C888/T80 SLN dispersion is also provided for comparison purposes. Ratio of the melting enthalpies ($\Delta H_{em}^T/\Delta H_{dis}$) of the emulsion systems presented in graph (a), representing the amount of crystalline material remaining within the emulsions post-processing (B). Identical lowercase letters indicate no significant differences between samples.

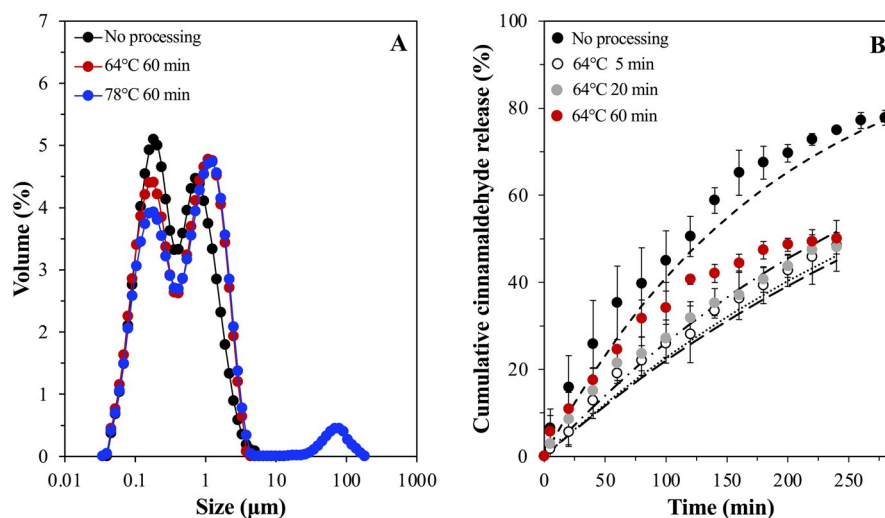


Figure 10. Droplet size distribution of C888/T80 SLN-stabilized emulsions before and after thermal processing at 64 and 78 °C for 60 min (a). *In vitro* release profile of cinnamaldehyde-loaded emulsions stabilized by C888/T80-SLNs after being subjected to thermal processing at 64 °C for varying durations (B). The profile of the respective emulsion system prior-sintering is also presented for comparison purposes. The interfacial barrier-limited model (Eq. (6)) fits to the data for the release of cinnamaldehyde from each emulsion system is also presented (— no processing, --- 64 °C 5 min, — 64 °C 20 min, - - - 64 °C 60 min).

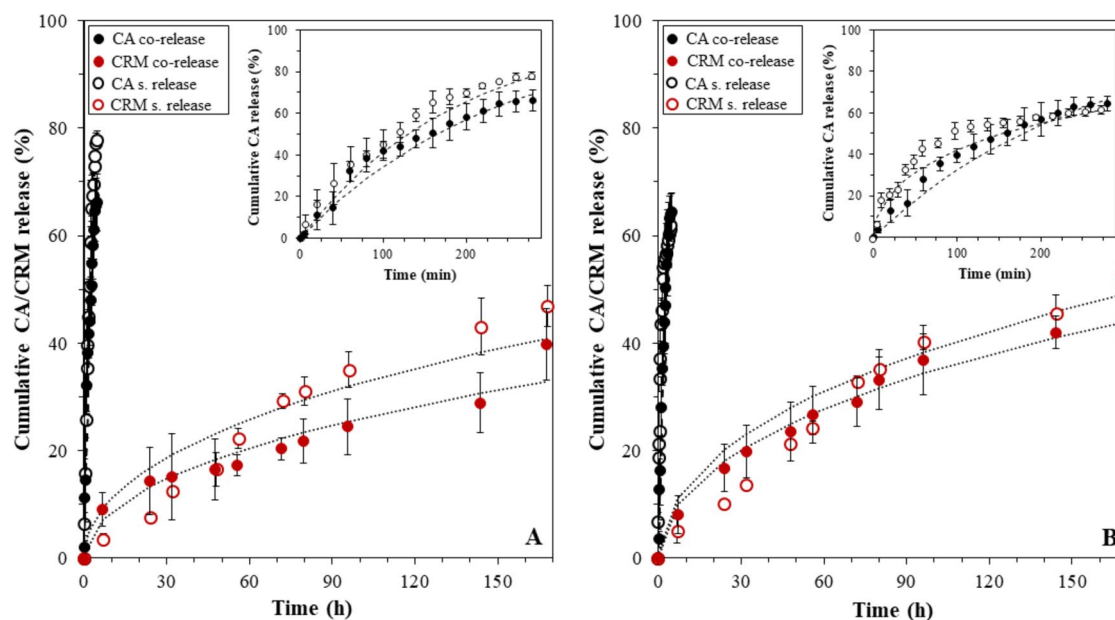


Figure 11. *In vitro* co-release profiles of cinnamaldehyde-loaded emulsion droplets stabilized by curcumin-loaded C888/T80-SLNs measured immediately after preparation (A) and after 1 month of emulsion storage (B). Data are presented at longer (main graph) and shorter (inset graph) timescales to demonstrate differences in the release rates. The Crank model (Eq. (3)) fitting for all curcumin data (dotted lines) and the interfacial barrier-limited model (Eq. (6)) fitting for all cinnamaldehyde curves (dashed lines) are also presented. For comparison purposes, the single release profiles of curcumin-loaded C888/T80-SLN-stabilized (blank) emulsions and CA-loaded emulsions stabilized by blank C888/T80 SLNs are included in both graphs.

time and temperature provides control over the porosity and roughness of the formed colloidosome shell, with smoother shells providing longer release times. The importance of the sintering conditions when it comes to the tightness and durability of Pickering emulsion-based colloidosomes was also highlighted in another work (Yin et al., 2017), whereby reduced oil leakage was recorded for tightly packed colloidosome layers at the interface. Correspondingly, Rao et al. (2009) demonstrated that longer sintering (3 h) of C888 matrices at 80 °C led to retarded release rate of ketorolac tromethamine, owing to the increased extent and firmness of the sintered structure.

Overall, the results presented here suggest that a level of particle sintering was attained following the thermal processing of the Pickering emulsions, although further work is required to better elucidate the effect of the chosen conditions. Amongst these could be the influence of the occurring interactions and type of bridges formed depending on the composition of the interfacial layer (i.e. co-existence or not of particles and surfactant molecules) (Johansson & Bergenstahl 1995). Additionally, a more detailed study on the combined effects of temperature and duration of the heating/sintering step could be carried out, particularly on shorter exposure periods to temperatures above the solid lipids' melting

temperature, that could potentially inform on the microstructural integrity of the formulation at critical conditions.

3.3. Co-release from lipid particle-stabilized emulsions

Having established the capability of both lipid particles and lipid particle-stabilized droplets to separately act as effective carriers and delivery systems of model hydrophobic actives, this part of the work scrutinized whether these performances perpetuated when the lipid-particle stabilized emulsion was utilized as a co-delivery platform. Previous work using lipid-particle stabilized emulsions as a co-delivery formulation has provided evidence that this type of carrier platform could indeed facilitate the independent co-delivery of actives by separately measuring their release behavior (Sakellari et al., 2021b). Herein, the co-release performance of cinnamaldehyde-loaded emulsion droplets stabilized by curcumin-loaded C888/T80 SLNs, was assessed by simultaneously acquiring the release profiles of the two actives under the same experimental conditions (Figure 11).

The co-release profiles for both curcumin (releasing from the C888/T80 SLNs) and cinnamaldehyde (discharging from the o/w droplets) showed no significant differences to the profiles that were individually acquired (Figure 11(A)). As was previously recorded, the highest percentage of cinnamaldehyde released over 280 min, while curcumin showed a relatively more sustained release rate with approximately 40% being released over the 7-day assessment. The D for CRM and k_1 constant for CA ($130 \times 10^{-20} \text{ cm}^2 \text{ s}^{-1}$ and $3.2 \times 10^{-15} \text{ cm}^2 \text{ s}^{-1}$, respectively) were in accordance with what was reported above for the singly measured release rates (see Tables 1 and 3, respectively). More importantly, the co-release behavior measured immediately after formation, was preserved even after 1 month of emulsion storage, with no major disparities being observed in the profiles or release kinetics ($D = 250 \times 10^{-20} \text{ cm}^2 \text{ s}^{-1}$ and $k_1 = 4.4 \times 10^{-15} \text{ cm}^2 \text{ s}^{-1}$) (Figure 11(B)). The co-encapsulation of the two actives did not alter the ability of either compartment in the formulation (i.e. lipid particles and emulsion droplets) to act as an independent active carrier, with no significant differences in the EE and LC values compared to the single encapsulation formulations.

4. Conclusions

The present study demonstrated the potential of SLN and NLC particles to simultaneously regulate the co-release performance of an active encapsulated within the particles themselves (acting as a carrier), but also that of a secondary active contained within the Pickering emulsion droplets (acting as a barrier). In terms of their identity as a carrier, investigation of the effect of changes to lipid particle formulation parameters, namely type of solid lipid and surfactant used, indicated that the release rate of the encapsulated active was predominantly governed by its relative location within the lipid matrix. Following confirmation of the Pickering stabilization capacity of the same particles, changes to their release control capability once within an emulsion setting were shown to be related to their formulation characteristics. The

compatibility between the particles' solid lipid and emulsion oil and the presence of surfactant micelles were suggested to have an inverse effect on the particles' ability to maintain control over the discharge of their active. In terms of their identity as a barrier, all particles, regardless of their composition, exhibited improved control compared to surfactant decorated interfaces, although the permeability of the interfacial layer appeared to greatly affect the release rate. In view of the latter, a post-production thermal approach was adopted to demonstrate that interfacial sintering of the particles and hence creation of a less permeable layer could enhance their barrier capacity and further impede active release from the droplets. Lastly, the hypothesis that each constituent of this system could extend its performance from the single to a dual release (co-release) setting, even when such markedly different individual release profiles (in terms of timescales) were chosen, was corroborated.

Overall, the results presented here underlined the aptitude of the developed Pickering emulsion platforms as promising systems for the compartmentalized co-encapsulation and independently controlled co-delivery of two actives, owing to their tunable lipid particle-decorated interfaces. Such modulation potential was manifested by the ability to effectively adjust the release profiles individually at a single active level, and then essentially transcribe these into a dual delivery platform. In terms of utility within the drug delivery arena, combining individual release profiles of shorter timescales could cater to co-delivery via an oral administration route, while more prolonged delivery profiles could be combined to develop long-acting injectables (Wilkinson et al., 2022) with a co-delivery capacity.

Author contributions

Georgia I. Sakellari: Conceptualization, Methodology, Formal analysis, Investigation, Writing – Original Draft; Hannah Batchelor: Conceptualization, Supervision, Writing – Review & Editing; Fotis Spyropoulos: Conceptualization, Supervision, Writing – Review & Editing, Funding acquisition. All authors have read and agreed to the published version of the manuscript.

Ethics statement

No ethical approval was required for this research.

Disclosure statement

No potential conflict of interest was reported by the authors.

Funding

This work was supported by funding from the Biotechnology and Biological Sciences Research Council (BBSRC) through the Midlands Integrative Bioscience Doctoral Training Partnership (BB/M01116X/1).

Data availability statement

The data that support the findings of this study are available from the corresponding author, [GIS], upon reasonable request.

References

- Alexandridis P, Holzwarth JF, Hatton TA. (1994). Micellization of poly(ethylene oxide)-poly(propylene oxide)-poly(ethylene oxide) triblock copolymers in aqueous solutions: thermodynamics of copolymer association. *Macromolecules* 27:2414–25. doi: [10.1021/ma00087a009](https://doi.org/10.1021/ma00087a009).
- Anantachaisilp S, Smith SM, Treetong A, et al. (2010). Chemical and structural investigation of lipid nanoparticles: drug–lipid interaction and molecular distribution. *Nanotechnology* 21:125102. doi: [10.1088/0957-4484/21/12/125102](https://doi.org/10.1088/0957-4484/21/12/125102).
- Awad A, Fina F, Trenfield SJ, et al. (2019). 3D printed pellets (miniprint-lets): a novel, multi-drug, controlled release platform technology. *Pharmaceutics* 11:148. doi: [10.3390/pharmaceutics11040148](https://doi.org/10.3390/pharmaceutics11040148).
- Badawi N, El-Say K, Attia D, et al. (2020). Development of pomegranate extract-loaded solid lipid nanoparticles: quality by design approach to screen the variables affecting the quality attributes and characterization. *ACS Omega* 5:21712–21. doi: [10.1021/acsomega.0C02618](https://doi.org/10.1021/acsomega.0C02618).
- Bertoni S, Passerini N, Albertini B. (2021). Liquid lipids act as polymorphic modifiers of tristearin-based formulations produced by melting technologies. *Pharmaceutics* 13:1089. doi: [10.3390/pharmaceutics13071089/51](https://doi.org/10.3390/pharmaceutics13071089/51).
- Brubach JB, Jannin V, Mahler B, et al. (2007). Structural and thermal characterization of glyceryl behenate by X-ray diffraction coupled to differential calorimetry and infrared spectroscopy. *Int J Pharm* 336:248–56. doi: [10.1016/j.ijpharm.2006.11.057](https://doi.org/10.1016/j.ijpharm.2006.11.057).
- Bunjes H. (2010). Lipid nanoparticles for the delivery of poorly water-soluble drugs. *J Pharm Pharmacol* 62:1637–45. doi: [10.1111/j.2042-7158.2010.01024.x](https://doi.org/10.1111/j.2042-7158.2010.01024.x).
- Čejková J, Štěpánek F. (2013). Compartmentalized and internally structured particles for drug delivery – a review. *Curr Pharm Des* 19:6298–314. doi: [10.2174/1381612811319350007](https://doi.org/10.2174/1381612811319350007).
- Chawda PJ, Shi J, Xue S, Young Quek S. (2017). Co-encapsulation of bioactives for food applications. *Food Quality Safety* 1:302–9. doi: [10.1093/fqsafe/fyx028](https://doi.org/10.1093/fqsafe/fyx028).
- Chen H, Dai H, Zhu H, et al. (2022). Construction of dual-compartmental micro-droplet via shrimp ferritin nanocages stabilized Pickering emulsions for co-encapsulation of hydrophobic/hydrophilic bioactive compounds. *Food Hydrocoll* 126:107443. doi: [10.1016/j.foodhyd.2021.107443](https://doi.org/10.1016/j.foodhyd.2021.107443).
- Crank J. (1975). *The mathematics of diffusion*. 2nd ed. London: Oxford University Press.
- Cui J, Sun C, Wang A, et al. (2020). Dual-functionalized pesticide nanocapsule delivery system with improved spreading behavior and enhanced bioactivity. *Nanomaterials* 10:220. doi: [10.3390/nano10020220](https://doi.org/10.3390/nano10020220).
- Deshmukh OS, Van Den Ende D, Stuart MC, et al. (2015). Hard and soft colloids at fluid interfaces: adsorption, interactions, assembly & rheology. *Adv Colloid Interface Sci* 222:215–27. doi: [10.1016/j.jcis.2014.09.003](https://doi.org/10.1016/j.jcis.2014.09.003).
- Dickinson E. (2010). Food emulsions and foams: stabilization by particles. *Curr Opin Colloid Interface Sci* 15:40–9. doi: [10.1016/j.cocis.2009.11.001](https://doi.org/10.1016/j.cocis.2009.11.001).
- Dinsmore AD, Hsu MF, Nikolaidis MG, et al. (2002). Colloidosomes: selectively permeable capsules composed of colloidal particles. *Science* 298:1006–9. doi: [10.1126/science.1074868](https://doi.org/10.1126/science.1074868).
- Frasch-Melnik S, Norton IT, Spyropoulos F. (2010). Fat-crystal stabilised w/o emulsions for controlled salt release. *J Food Eng* 98:437–42. doi: [10.1016/j.jfoodeng.2010.01.025](https://doi.org/10.1016/j.jfoodeng.2010.01.025).
- Frelichowska J, Bolzinger MA, Pelletier J, et al. (2009a). Topical delivery of lipophilic drugs from o/w Pickering emulsions. *Int J Pharm* 371:56–63. doi: [10.1016/j.ijpharm.2008.12.017](https://doi.org/10.1016/j.ijpharm.2008.12.017).
- Frelichowska J, Bolzinger MA, Valour P, et al. (2009b). Pickering w/o emulsions: drug release and topical delivery. *Int J Pharm* 368:7–15. doi: [10.1016/j.ijpharm.2008.09.057](https://doi.org/10.1016/j.ijpharm.2008.09.057).
- Garrec DA, Frasch-Melnik S, Henry JVL, et al. (2012). Designing colloidal structures for micro and macro nutrient content and release in foods. *Faraday Discuss* 158:37–49. doi: [10.1039/c2fd20024d](https://doi.org/10.1039/c2fd20024d).
- Gordillo-Galeano A, Ponce A, Mora-Huertas CE. (2022). In vitro release behavior of SLN, NLC, and NE: an explanation based on the particle structure and carried molecule location. *J Drug Deliv Sci Technol* 76:103768. doi: [10.1016/j.jddst.2022.103768](https://doi.org/10.1016/j.jddst.2022.103768).
- Graily Moradi F, Hejazi MJ, Hamishehkar H, Enayati AA. (2019). Co-encapsulation of imidacloprid and lambda-cyhalothrin using biocompatible nanocarriers: characterization and application. *Ecotoxicol Environ Saf* 175:155–63. doi: [10.1016/j.ecoenv.2019.02.092](https://doi.org/10.1016/j.ecoenv.2019.02.092).
- Guy RH, Hadgraft J, Kellaway IW, Taylor M. (1982). Calculations of drug release rates from particles. *Int J Pharm* 11:199–207. doi: [10.1016/0378-5173\(82\)90038-2](https://doi.org/10.1016/0378-5173(82)90038-2).
- Han L, Lu K, Zhou S, et al. (2021). Development of an oil-in-water emulsion stabilized by a black bean protein-based nanocomplex for co-delivery of quercetin and perilla oil. *LWT* 138:110644. doi: [10.1016/j.lwt.2020.110644](https://doi.org/10.1016/j.lwt.2020.110644).
- Han F, Luo D, Qu W, et al. (2020). Nanoliposomes codelivering bioactive peptides produce enhanced anti-aging effect in human skin. *J Drug Deliv Sci Technol* 57:101693. doi: [10.1016/j.jddst.2020.101693](https://doi.org/10.1016/j.jddst.2020.101693).
- Helal NA, Eassa HA, Amer AM, et al. (2019). Nutraceuticals' novel formulations: the good, the bad, the unknown and patents involved. *Recent Pat Drug Deliv Formul* 13:105–56. doi: [10.2174/1872211313666190503112040](https://doi.org/10.2174/1872211313666190503112040).
- Hu L, Tang X, Correspondence C, et al. (2004). Solid lipid nanoparticles (SLNs) to improve oral bioavailability of poorly soluble drugs. *J Pharm Pharmacol* 56:1527–35. doi: [10.1211/0022357044959](https://doi.org/10.1211/0022357044959).
- Jamieson GS, Baughman WF. (1922). The chemical composition of sunflower-seed oil. *J Am Chem Soc* 44:2952–7. doi: [10.1021/ja01433a036](https://doi.org/10.1021/ja01433a036).
- Jenning V, Thünemann AF, Gohla SH. (2000). Characterisation of a novel solid lipid nanoparticle carrier system based on binary mixtures of liquid and solid lipids. *Int J Pharm* 199:167–77. doi: [10.1016/S0378-5173\(00\)00378-1](https://doi.org/10.1016/S0378-5173(00)00378-1).
- Johansson D, Bergenstahl B. (1995). Sintering of fat crystal networks in oil during post-crystallization processes. *J Am Oil Chem Soc* 72:911–20. doi: [10.1007/BF02542069](https://doi.org/10.1007/BF02542069).
- Jores K, Haberland A, Wartewig S, et al. (2005). Solid lipid nanoparticles (SLN) and oil-loaded SLN studied by spectrofluorometry and Raman spectroscopy. *Pharm Res* 22:1887–97. doi: [10.1007/s11095-005-7148-5](https://doi.org/10.1007/s11095-005-7148-5).
- Jores K, Mehnert W, Drechsler M, et al. (2004). Investigations on the structure of solid lipid nanoparticles (SLN) and oil-loaded solid lipid nanoparticles by photon correlation spectroscopy, field-flow fractionation and transmission electron microscopy. *J Control Release* 95:217–27. doi: [10.1016/j.jconrel.2003.11.012](https://doi.org/10.1016/j.jconrel.2003.11.012).
- Jores K, Mehnert W, Mäder K. (2003). Physicochemical investigations on solid lipid nanoparticles and on oil-loaded solid lipid nanoparticles: a nuclear magnetic resonance and electron spin resonance study. *Pharm Res* 20:1274–83. doi: [10.1023/a:1025065418309](https://doi.org/10.1023/a:1025065418309).
- Kim MR, Feng T, Zhang Q, et al. (2019). Co-encapsulation and co-delivery of peptide drugs via polymeric nanoparticles. *Polymers (Basel)* 11(2), 288. doi: [10.3390/polym11020288](https://doi.org/10.3390/polym11020288).
- Kishore N, Dhanalekshmi UM, Raja D, et al. (2011). Design and in vitro evaluation of solid-lipid nanoparticle drug delivery for aceclofenac. *Journal of Dispersion Science and Technology*, 33(1), 96–102. doi: [10.1080/01932691.2010.534293](https://doi.org/10.1080/01932691.2010.534293).
- Kolishetti N, Dhar S, Valencia PM, et al. (2010). Engineering of self-assembled nanoparticle platform for precisely controlled combination drug therapy. *Proc Natl Acad Sci USA* 107:17939–44. doi: [10.1073/pnas.1011368107](https://doi.org/10.1073/pnas.1011368107).
- Kurukji D, Norton I, Spyropoulos F. (2016). Fabrication of sub-micron protein-chitosan electrostatic complexes for encapsulation and pH-modulated delivery of model hydrophilic active compounds. *Food Hydrocoll* 53:249–60. doi: [10.1016/j.foodhyd.2015.02.021](https://doi.org/10.1016/j.foodhyd.2015.02.021).
- Lee HG, Park YS, Jeong JH, et al. (2019). Physicochemical properties and drug-release mechanisms of dual-release bilayer tablet containing mirabegron and fesoterodine fumarate. *Drug Des Devel Ther* 13:2459–74. doi: [10.2147/dddt.s212520](https://doi.org/10.2147/dddt.s212520).
- Li N, Zhao L, Qi L, et al. (2016). Polymer assembly: promising carriers as co-delivery systems for cancer therapy. *Prog Polym Sci* 58:1–26. doi: [10.1016/j.progpolymsci.2015.10.009](https://doi.org/10.1016/j.progpolymsci.2015.10.009).
- Liu J, Chi D, Pan S, et al. (2019). Effective co-encapsulation of doxorubicin and irinotecan for synergistic therapy using liposomes prepared with

- triethylammonium sucrose octasulfate as drug trapping agent. *Int J Pharm* 557:264–72. doi: [10.1016/j.ijpharm.2018.12.072](https://doi.org/10.1016/j.ijpharm.2018.12.072).
- Luo YF, Chen DW, Ren LX, et al. (2006). Solid lipid nanoparticles for enhancing vinpocetine's oral bioavailability. *J Control Release* 114:53–9. doi: [10.1016/j.jconrel.2006.05.010](https://doi.org/10.1016/j.jconrel.2006.05.010).
- Macridachis-González J, Bayés-García L, Calvet T. (2020). An insight into the solid-state miscibility of triacylglycerol crystals. *Molecules* 25:4562. doi: [10.3390/molecules25194562](https://doi.org/10.3390/molecules25194562).
- McClements DJ, Dungan SR. (1993). Factors that affect the rate of oil exchange between oil-in-water emulsion droplets stabilized by a non-ionic surfactant: droplet size, surfactant concentration, and ionic strength. *J Phys Chem* 97:7304–8. doi: [10.1021/j100130a030](https://doi.org/10.1021/j100130a030).
- McClements DJ, Dungan SR, German JB, Kinsella JE. (1993a). Evidence of oil exchange between oil-in-water emulsion droplets stabilized by milk proteins. *J Coll Interf Sci* 156:425–9. doi: [10.1006/jcis.1993.1133](https://doi.org/10.1006/jcis.1993.1133).
- McClements DJ, Dungan SR, German JB, Kinsella JE. (1993b). Factors which affect oil exchange between oil-in-water emulsion droplets stabilized by whey protein isolate: protein concentration, droplet size and ethanol. *Colloids Surf A Physicochem Eng Asp* 81:203–10. doi: [10.1016/0927-7757\(93\)80247-c](https://doi.org/10.1016/0927-7757(93)80247-c).
- Meng J, Guo F, Xu H, et al. (2016). Combination therapy using co-encapsulated resveratrol and paclitaxel in liposomes for drug resistance reversal in breast cancer cells in vivo. *Sci Rep* 6:22390. doi: [10.1038/srep22390](https://doi.org/10.1038/srep22390).
- Ming Y, Xia Y, Ma G, Xia CY. (2022). Aggregating particles on the O/W interface: Tuning Pickering emulsion for the enhanced drug delivery systems. *Aggregate* 3:e162. doi: [10.1002/agt2.162](https://doi.org/10.1002/agt2.162).
- Motevalli SM, Eltahan AS, Liu L, et al. (2019). Co-encapsulation of curcumin and doxorubicin in albumin nanoparticles blocks the adaptive treatment tolerance of cancer cells. *Biophys Rep* 5:19–30. doi: [10.1007/s41048-018-0079-6](https://doi.org/10.1007/s41048-018-0079-6).
- Noack A, Hause G, Mäder K. (2012). Physicochemical characterization of curcuminoid-loaded solid lipid nanoparticles. *Int J Pharm* 423:440–51. doi: [10.1016/j.ijpharm.2011.12.011](https://doi.org/10.1016/j.ijpharm.2011.12.011).
- Prestidge CA, Simovic S. (2006). Nanoparticle encapsulation of emulsion droplets. *Int J Pharm* 324:92–100. doi: [10.1016/j.ijpharm.2006.06.044](https://doi.org/10.1016/j.ijpharm.2006.06.044).
- Rao M, Ranpise A, Borate S, Thanki K. (2009). Mechanistic evaluation of the effect of sintering on Compritol® 888 ATO matrices. *AAPS PharmSciTech* 10:355–360. doi: [10.1208/s12249-009-9211-8](https://doi.org/10.1208/s12249-009-9211-8).
- Rosenblatt KM, Bunjes H. (2009). Poly(vinyl alcohol) as emulsifier stabilizes solid triglyceride drug carrier nanoparticles in thea-modification. *Mol Pharm* 6:105–20. doi: [10.1021/MP8000759](https://doi.org/10.1021/MP8000759).
- Sakellari GI, Zafeiri I, Batchelor H, Spyropoulos F. (2021a). Formulation design, production and characterisation of solid lipid nanoparticles (SLN) and nanostructured lipid carriers (NLC) for the encapsulation of a model hydrophobic active. *Food Hydrocoll Health* 1:None. doi: [10.1016/j.fhfh.2021.100024](https://doi.org/10.1016/j.fhfh.2021.100024).
- Sakellari GI, Zafeiri I, Batchelor H, Spyropoulos F. (2022). Solid lipid nanoparticles and nanostructured lipid carriers of dual functionality at emulsion interfaces. Part I: Pickering stabilisation functionality. *Colloids Surf A Physicochem Eng Asp* 654:130135. doi: [10.1016/j.colsurfa.2022.130135](https://doi.org/10.1016/j.colsurfa.2022.130135).
- Sakellari GI, Zafeiri I, Batchelor H, Spyropoulos F. (2023). Solid lipid nanoparticles and nanostructured lipid carriers of dual functionality at emulsion interfaces. Part II: active carrying/delivery functionality. *Colloids Surf A Physicochem Eng Asp* 659:130787. doi: [10.1016/j.colsurfa.2022.130787](https://doi.org/10.1016/j.colsurfa.2022.130787).
- Sakellari GI, Zafeiri I, Pawlik A, et al. (2021b). Independent co-delivery of model actives with different degrees of hydrophilicity from oil-in-water and water-in-oil emulsions stabilised by solid lipid particles via a Pickering mechanism: a-proof-of-principle study. *J Colloid Interface Sci* 587:644–9. doi: [10.1016/j.jcis.2020.11.021](https://doi.org/10.1016/j.jcis.2020.11.021).
- Salminen H, Gömmel C, Leuenberger BH, Weiss J. (2016). Influence of encapsulated functional lipids on crystal structure and chemical stability in solid lipid nanoparticles: towards bioactive-based design of delivery systems. *Food Chem* 190:928–37. doi: [10.1016/j.foodchem.2015.06.054](https://doi.org/10.1016/j.foodchem.2015.06.054).
- Salminen H, Helgason T, Aulbach S, et al. (2014). Influence of co-surfactants on crystallization and stability of solid lipid nanoparticles. *J Colloid Interface Sci* 426:256–63. doi: [10.1016/j.jcis.2014.04.009](https://doi.org/10.1016/j.jcis.2014.04.009).
- Samtlebe M, Yucel U, Weiss J, Coupland JN. (2012). Stability of solid lipid nanoparticles in the presence of liquid oil emulsions. *J Am Oil Chem Soc* 89:609–17. doi: [10.1007/s11746-011-1944-3](https://doi.org/10.1007/s11746-011-1944-3).
- Shah M, Agrawal YK, Garala K, Ramkishan A. (2012). Solid lipid nanoparticles of a water soluble drug, ciprofloxacin hydrochloride. *Indian J Pharm Sci* 74:434–42. doi: [10.4103/0250-474x.108419](https://doi.org/10.4103/0250-474x.108419).
- Shahani K, Panyam J. (2011). Highly loaded, sustained-release microparticles of curcumin for chemoprevention. *J Pharm Sci* 100:2599–609. doi: [10.1002/JPS.22475](https://doi.org/10.1002/JPS.22475).
- Shrimal P, Jadeja G, Patel S. (2020). A review on novel methodologies for drug nanoparticle preparation: Microfluidic approach. *Chem Eng Res Des* 153:728–56. doi: [10.1016/j.cherd.2019.11.031](https://doi.org/10.1016/j.cherd.2019.11.031).
- Simovic S, Prestidge CA. (2007). Nanoparticle layers controlling drug release from emulsions. *Eur J Pharm Biopharm* 67:39–47. doi: [10.1016/j.elpbj.2007.01.011](https://doi.org/10.1016/j.elpbj.2007.01.011).
- Souto EB, Mehnert W, Müller RH. (2006). Polymorphic behaviour of Compritol®888 ATO as bulk lipid and as SLN and NLC. *J Microencapsul* 23:417–33. doi: [10.1080/02652040600612439](https://doi.org/10.1080/02652040600612439).
- Spyropoulos F, Clarke C, Kurukji D, et al. (2020). Emulsifiers of Pickering-like characteristics at fluid interfaces: impact on oil-in-water emulsion stability and interfacial transfer rate kinetics for the release of a hydrophobic model active. *Colloids Surf A Physicochem Eng Asp* 607:125413. doi: [10.1016/j.colsurfa.2020.125413](https://doi.org/10.1016/j.colsurfa.2020.125413).
- Spyropoulos F, Kurukji D, Taylor P, Norton IT. (2018). Fabrication and utilization of bifunctional protein/polysaccharide coprecipitates for the independent codelivery of two model actives from simple oil-in-water emulsions. *Langmuir* 34:3934–48. doi: [10.1021/acs.langmuir.7b04315](https://doi.org/10.1021/acs.langmuir.7b04315).
- Sun Y, Tang W, Pu C, et al. (2022). Improved stability of liposome-stabilized emulsions as a co-encapsulation delivery system for vitamin B2, vitamin E and β -carotene. *Food Funct* 13:2966–84. doi: [10.1039/d1fo03617c](https://doi.org/10.1039/d1fo03617c).
- Tavano L, Muzzalupo R, Picci N, de Cindio B. (2014). Co-encapsulation of antioxidants into niosomal carriers: gastrointestinal release studies for nutraceutical applications. *Colloids Surf B Biointerfaces* 114:82–8. doi: [10.1016/j.colsurfb.2013.09.058](https://doi.org/10.1016/j.colsurfb.2013.09.058).
- Tiyaboonchai W, Tungpradit W, Plianbangchang P. (2007). Formulation and characterization of curcuminoids loaded solid lipid nanoparticles. *Int J Pharm* 337:299–306. doi: [10.1016/J.IJPHARM.2006.12.043](https://doi.org/10.1016/J.IJPHARM.2006.12.043).
- Ugazio E, Cavalli R, Gasco MR. (2002). Incorporation of cyclosporin A in solid lipid nanoparticles (SLN). *Int J Pharm* 241:341–4. doi: [10.1016/S0378-5173\(02\)00268-5](https://doi.org/10.1016/S0378-5173(02)00268-5).
- Venkateswarlu V, Manjunath K. (2004). Preparation, characterization and in vitro release kinetics of clozapine solid lipid nanoparticles. *J Control Release* 95:627–38. doi: [10.1016/j.jconrel.2004.01.005](https://doi.org/10.1016/j.jconrel.2004.01.005).
- Wang J, Hao H, Cai JH. (2019). Amphiphilic drug delivery microcapsules via layer-by-layer self-assembly. *J Macromol Sci Pt B* 58:535–50. doi: [10.1080/00222348.2019.1593640](https://doi.org/10.1080/00222348.2019.1593640).
- Washington C, Evans K. (1995). Release rate measurements of model hydrophobic solutes from submicron triglyceride emulsions. *J Control Release* 33:383–90. doi: [10.1016/0168-3659\(94\)00110-G](https://doi.org/10.1016/0168-3659(94)00110-G).
- Wei Y, Yang S, Zhang L, et al. (2020). Fabrication, characterization and in vitro digestion of food grade complex nanoparticles for co-delivery of resveratrol and coenzyme Q10. *Food Hydrocoll* 105:105791. doi: [10.1016/j.foodhyd.2020.105791](https://doi.org/10.1016/j.foodhyd.2020.105791).
- Weiss J, McClements DJ. (2000). Mass transport phenomena in oil-in-water emulsions containing surfactant micelles: solubilization. *Langmuir* 16:5879–83. doi: [10.1021/la9914763](https://doi.org/10.1021/la9914763).
- Wilkinson J, Ajulo D, Tamburrini V, et al. (2022). Lipid based intramuscular long-acting injectables: current state of the art. *Eur J Pharm Sci* 178:106253. doi: [10.1016/J.EJPS.2022.106253](https://doi.org/10.1016/J.EJPS.2022.106253).
- Yin D, Bai L, Jia Y, et al. (2017). Microencapsulation through thermally sintering Pickering emulsion-based colloidosomes. *Soft Matter* 13:3720–5. doi: [10.1039/C7SM00528H](https://doi.org/10.1039/C7SM00528H).
- Yow HN, Routh AF. (2009). Release profiles of encapsulated actives from colloidosomes sintered for various durations. *Langmuir* 25:159–66. doi: [10.1021/la802711y](https://doi.org/10.1021/la802711y).

- Zafeiri I, Norton JE, Smith P, et al. (2017a). The role of surface active species in the fabrication and functionality of edible solid lipid particles. *J Colloid Interface Sci* 500:228–40. doi: [10.1016/j.jcis.2017.03.085](https://doi.org/10.1016/j.jcis.2017.03.085).
- Zafeiri I, Smith P, Norton IT, Spyropoulos F. (2017b). Fabrication, characterisation and stability of oil-in-water emulsions stabilised by solid lipid particles: the role of particle characteristics and emulsion microstructure upon Pickering functionality. *Food Funct* 8:2583–91. doi: [10.1039/c7fo00559h](https://doi.org/10.1039/c7fo00559h).
- Zhao W, Yan Y, Chen X, Wang T. (2022a). Combining printing and nanoparticle assembly: methodology and application of nanoparticle patterning. *The Innovation* 3:100253. doi: [10.1016/J.XINN.2022.100253](https://doi.org/10.1016/J.XINN.2022.100253).
- Zhao W, Zeng M, Li K, et al. (2022b). Solid lipid nanoparticle as an effective drug delivery system of a novel curcumin derivative: formulation, release in vitro and pharmacokinetics in vivo 60:2300–7. doi: [10.1080/13880209.2022.2136205](https://doi.org/10.1080/13880209.2022.2136205).
- Zur Mühlen A, Schwarz C, Mehnert W. (1998). Solid lipid nanoparticles (SLN) for controlled drug delivery – drug release and release mechanism. *Eur J Pharm Biopharm* 45:149–55. doi: [10.1016/s0939-6411\(97\)00150-1](https://doi.org/10.1016/s0939-6411(97)00150-1).